A PROPOSAL FOR A CRYSTAL-BALL DETECTOR SYSTEM

D. Habs, F. S. Stephens, and R. M. Diamond

March 1979

Prepared for the U. S. Department of Energy
under Contract no. W-7405-ENG-48

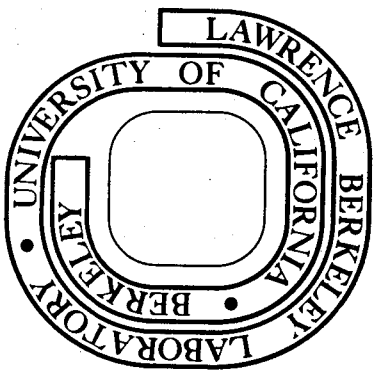

DISCLAIMER

A PROPOSAL FOR A CRYSTAL-BALL DETECTOR SYSTEM

D. Habs

University of Heidelberg
Heidelberg, W.Germany

F. S. Stephens and R. M. Diamond

Lawrence Berkeley Laboratory
University of California
Berkeley, California 94720

March 1979

This work was supported by the U. S. Department of Energy

3-79/130

Index

ABSTRACT

The interest in highly excited nuclei with large angular momentum has prompted this proposal of a universal γ-ray spectrometer (called the Crystal Ball) consisting of a 4π modularized NaI(Tl) detector system with 162 elements of equal solid angle. The proposed detector has an overall spherical shape with an inner radius of 22.86 cm and an outer radius of 38.10 cm. The major experimental quantities to be measured are:

a) Gamma-ray multiplicity, with about 20% resolution in an event-by-event mode. This allows for the first time the measurement of multiplicity spectra, while up to now only moments of multiplicity distributions have been determined. The multiplicity is closely related to the spin of the nucleus.

b) Total energy of the gamma rays, with about 20% resolution for a total energy of 30 MeV in an event-by-event mode.

c) Gamma-ray angular distributions, with an angular resolution of about $\pm 9°$ in an event-by-event mode. The direction of the spin of the nucleus and the multipolarities of the γ-ray transitions can be deduced from the angular distribution.

d) The energies of individual gamma rays, with about 7% resolution for 1 MeV transitions. The spectrum of individual γ rays is distorted by pile-up in the crystal and Compton scattering between crystals. To reduce the former effect requires a large number of crystals compared to the number of γ-rays, and only a few crystals per event which show no hits in any neighbor crystal avoid the second problem.

In a more general way the high efficiency, the tolerance of high counting rates and the good time resolution (2-3 ns) of the spectrometer allow

the selection of special events in more elaborate coincidence experiments with additional counters.

A detailed test of a prototype section consisting of six NaI(Tl) detectors is planned for 1979, and as a result of these tests, the optimum configuration will be chosen. The total system could be in operation by 1981. Usage at the 88" Cyclotron as well as at the SuperHILAC accelerator is anticipated.

A March, 1979 price estimate for the total system is $600K, divided into 332K$ for the NaI detector system itself, 140K$ for electronics and cables, 97K$ for support frame and scattering chamber, and 30K$ for contingencies. In addition, it is estimated that one man-year of programming help will be needed from operating money.

The proposal is organized in four sections:

I) scientific justification for this universal γ-ray spectrometer,

II) an explanation of the special design of the Crystal Ball,

III) a description of the components of the total system,

IV) the time schedule and budget.

I. SCIENTIFIC JUSTIFICATION

A. Requirements

The study of electromagnetic radiation, or gamma rays, is one of our most important sources of information about nuclear systems. The systematics of the energy of individual γ-ray transitions is generally closely related to the structure of the emitting states, and its study has always been one of the principal branches of nuclear spectroscopy. An obvious example would be the observation of a cascade of γ-ray transitions, each differing by a constant amount of energy from the one preceding it. This would be a clear signal of a rotational cascade from a deformed nucleus. But also the total energy emitted as γ rays is important; it defines an "entry point" in the excitation energy-angular momentum surface where electromagnetic radiation takes over from other decay processes. The locus of such points for different angular momenta, the entry line,[1,2] gives information both about the nuclear structure and about the mechanism of the preceding decay processes. Such studies are relatively new, but have already been used with heavy-ion compound nucleus (HICN) reactions to give moments of inertia at very high spin values.[3] The angular correlation and polarization of γ rays contain information both about the orientation (including the alignment) of the angular momentum of the emitting nucleus and about the multipolarity of the observed γ rays.[4,5] The alignment of the nucleus has recently become a lively topic in deep-inelastic collision (DIC) studies and discussions, as the expected alignment does not always appear in all types of measurements.[6-9] Determination of γ-ray multipolarity by angular correlation studies[4] has recently been used to identify rotational behavior following

the HICN events. The total number of γ rays emitted, the multiplicity, can be large, and when it exceeds ten or so it very likely is due to the high total angular momentum of the emitting system.[3,10-12] The exact relationship between multiplicity and total angular momentum after particle emission varies in different cases, but for the broad class of rotational nuclei it is approximately just a factor of two -- essentially all electric quadrupole transitions removing two units of angular momentum. More accurately it can be expressed as $I = (M-\delta)2$, where δ stands for the 3-4 statistical transitions that carry away essentially zero spin. Since the total angular momentum is an important quantity in the study of both nuclear structure and reaction mechanisms (particularly for deep-inelastic collisions), the measurement of the γ-ray multiplicity is now quite important. A final parameter involved in γ-ray measurements is their time of emission. This is used to relate the observed γ ray to other γ rays or decay processes, and often is essential for its proper identification. These four quantities, the energy, both individual and total, the angular correlation and polarization, the number of γ rays, and the time of emission, are the information that we can presently obtain from nuclear electromagnetic radiation, and the purpose of this proposal is to build an instrument to measure simultaneously as many of these quantities as possible with reasonable accuracy.

It is important to distinguish between a "complete" measurement of one of these quantities on an event-by-event basis, and an "incomplete" measurement which can only be related statistically to a value or set of values for that quantity. Only in the former case (whether or not a calculation is involved) can events be selected (gates set) which

correspond to any desired value for that quantity. This is not possible in the latter case, even if the observed distribution of values for the measured events can be uniquely connected to the true distribution. Consider the multiplicity, for example. Information from an array of, say, ten detectors can be statistically related to the first ten moments of the multiplicity distribution, which will normally define this distribution rather well. Yet a single event, in which six detectors fire, cannot be uniquely related to any particular multiplicity. That is, those events having exactly multiplicity six cannot be selected. Rather, a particular measurement (six detectors fire) corresponds, with a certain probability distribution, to a range of multiplicity values from six on up. If, on the other hand, the space surrounding the emitting nucleus is completely filled with a large number of detectors, the true number of γ-rays given out event-by-event can be determined, within a certain "resolution" caused by experimental difficulties, such as Compton scattering between counters and multiple hits in the same counter. It is of crucial importance that this resolution be sufficiently good for all the quantities we want to measure, since otherwise we do not realize the full power of event-by-event multi-dimensional storage of the measured parameters.

B. Instrument

With these requirements in mind, the general features of an ultimate γ-ray detector are surprisingly clear. For reasonable resolution of total energy we need a high efficiency for the γ rays; this means the detector must subtend a large fraction of the total solid angle (4π) and not be significantly transparent to the original γ rays or to their Compton-

scattered secondaries. For a cascade of thirty 1 MeV γ-ray transitions, total efficiencies of 0.5, 0.7, and 0.9 give resolutions, (FWHM) divided by the value at the maximum, of 61%, 34%, and 15%, respectively. Presently operating total-energy spectrometers have efficiencies up to about 0.8 (of 4π), and the resolution obtained has proved valuable in several contexts: resolving reaction channels in heavy-ion compound-nucleus reactions, defining entry lines for γ-ray emission, establishing the connection between total energy and angular momentum, and in discriminating against low total-energy events like radioactive decays, transfer reactions, and Coulomb excitation. As good, or better, resolution would be clearly desirable, so we must aim at an efficiency of ≥ 0.8, implying a spherical shell of NaI, having a thickness of 15-18 cm. To avoid multiple γ rays hitting one detector in the same event, we need many detectors. The number, N, must be large compared with the maximum multiplicity, M_{max}, we anticipate measuring. Already multiplicities following (HI,x$n\gamma$) reactions have been measured between 30-35. The deep-inelastic reactions with two γ-emitting fragments, will surely go beyond values of 50 in some cases. Since we want $N \gg M_{max}$, we must have $N > 100$. The detailed analysis in Section II of this proposal suggests N = 122 or 162. In such cases the multiplicity resolution will be 20-25% compared with the best so far obtained by any method of ~70%. This is an important gain, since it implies a corresponding resolution in the angular momentum. The shell of NaI detectors will need an inner radius large enough to allow separation by time-of-flight of the γ rays from all particles ($v/c \sim 0.1$), particularly neutrons, that might be emitted from a reaction. Since the time resolution achievable with NaI detectors is 2-3 ns, a distance from target to detectors of 22-25 cm would give a difference

in flight-time of 6-7 ns. This is about the minimum to achieve such a separation. With such an inner radius for the NaI shell, the diameter of the inner face of each counter (for a 162 counter system) is ~7 cm, so that they subtend a half-angle of ~9°. Thus an event can be localized to ±9° by the system, which is adequate for most angular correlation purposes.

So, to recapitulate, we need a spherical shell of NaI with an inner radius of 22-25 cm and an outer radius of ~40 cm, divided into 162 detectors of equal solid angle. This would give on an event-by-event basis: total γ-ray energy to 20%, γ-ray multiplicity to 20%, the angle of emission of a γ ray to ±9°, and time resolution of 2-3 ns. It would not give polarization information in any simple way, and more unfortunately, it does not uniformly give individual γ-ray energies with good resolution. This is because Compton scattering and multiple γ-ray hits in the same detector smear out considerably the individual γ-ray energies. The true spectrum can be recovered on the average by unfolding, and some gating selection can be made (setting of lower-energy limits, for example). A few counters, those that show no hits in any neighbor counter, can yield true γ-ray energies (though the problem of multiple hits remains). The number of such "anti-Compton" type counters increases with the total number of counters, thus favoring the larger number. However, even with 122 detectors, the "crystal ball" far exceeds anything now existing in its ability to extract information associated with γ-ray de-excitation. We should note the large store of information already available on the Stanford crystal ball[13] and a proposal for a smaller instrument by D. G. Sarantites.[14]

C. Experiments

There are many problems that will benefit from studies using the crystal ball and associated counters, and the present section will provide a few illustrations. There are certainly very interesting and relevant experiments that could be done with the crystal ball alone, and a number of examples have already been given above. One more that might be mentioned is to measure, not just the average entry line in a heavy-ion, xnγ reaction, but the full three-dimensional distribution of intensity, angular momentum (multiplicity), and total γ-ray energy. Furthermore, at each point of this distribution, the angular correlation of the γ-rays will give information about the nuclear structure along the decay pathway to the ground state.

Nevertheless, the ease of adding other types of detectors to obtain additional information at relatively little cost will make such more complex experiments very attractive relative to ones using the crystal ball alone. So further discussion will be divided, somewhat arbitrarily, into two parts: the first involves removing one or a few individual NaI counters from the ball and replacing them with other types of detectors, and the second involves placing the additional detectors inside the crystal ball.

The removal of one counter from the shell will open an area about 7 cm in diameter on the inner sphere, and cost 0.6% in NaI solid angle (for a ball of 162 counters). Several such counters can be removed (for example, at selected angles) before the solid-angle loss becomes serious. Such an opening can accommodate a Ge detector, which, if mounted in a long snout, could be pushed in quite close to

the target (center). These counters have a high resolution for γ-ray energies, and insofar as there are resolved γ-ray lines in the spectrum, can detect them with reasonable efficiency (a few percent). This can be used to identify the product nucleus provided its γ-ray lines are known. In the HICN reactions the reaction channel can thus be identified, and all the crystal ball information sorted event-by-event for each reaction channel. Comparison of different channels gives detailed information on the reaction mechanism. Likewise in transfer reactions, a particular product can readily be selected (as can only be done with great difficulty to a mass resolution of one for medium and heavy nuclei by time-of-flight) and information on its cross section, spin, entry line, and nuclear structure is provided by the crystal ball. In deep-inelastic collisions (DIC), one might want to make selection on the total energy or multiplicity to try to resolve lines in the Ge spectrum (not heretofore done) and thus identify specific product nuclei. In somewhat more detail, one could go into the HICN products, where the appropriate γ rays are known, and study the population leading to various excited states (the side-feeding properties) having different spin, energy, etc. Nuclear structure studies could be greatly helped by obtaining Ge spectra and Ge-Ge coincidence spectra, when selections are made on angular momentum (multiplicity) total energy, or spin alignment (from the angular correlation of the coincident γ-rays) as given by the coincident crystal-ball channel. In HICN reactions one could select the highest angular-momentum states, for example, and study their γ-ray transitions, and hence learn about the structure of these states. One might even hope to resolve the γ-ray continuum in favorable cases by suitable gates on multiplicity and total energy. Also in Coulomb-excitation studies the placement in the level

scheme of a γ ray resolved in the Ge detector should be given by the associated crystal ball data. Still other examples could be given for the Ge detector-crystal ball system.

A large NaI crystal, shielded except in the center of one face, would have a response function good enough to give individual γ-ray energies event-by-event. This detector could look through an opening in the crystal ball provided by removal of one of the crystal ball's counters. This would permit the selection of yrast "bump" transitions, for example, following HICN reactions, and would allow the determination of the multiplicities and total energies associated with such transitions. The highest-energy bump transitions are generally stretched E2 transitions between states of very high spin, and their study can provide information about these states (especially their moments of inertia). Such transitions might be sought following DIC events also, and if observed would indicate a large conversion of orbital to internal angular momentum.

The area opened up by the removal of one, two, or even several crystal-ball counters can also be covered by position-sensitive avalanche counters for particle detection. Two such counters (which can give the position of charged particles to ~0.2 mm and time to 0.3 ns) can identify the products (mass and energy) of a two-body breakup following a heavy-ion collision. (To obtain a good velocity measurement by time-of-flight, these counters must be placed sufficiently distant from the target, and, in particular, outside the crystal ball.) In transfer reactions and in Coulomb excitation, the direction of the recoiling fragments, as determined by the avalanche counters, can be used to correct the Doppler shift of the coincident γ-ray lines observed in a Ge detector, thus considerably improving the resultant resolution. The combination of the position-

sensitive detectors followed by particle total-energy detectors (ionization chambers, for example) would give virtually complete kinematic information on the products of most heavy-ion reactions. The crystal-ball information on the γ-rays' total energy, multiplicity, angular correlation, and time distribution can then be studied for the selected type of heavy-ion reaction. Such information can now be taken only in part, and even so would involve several bombardments with different NaI arrangements.

Neutron counters can also be positioned at the openings to determine the energy and angle of the emitted neutrons. It would be possible to search for fast neutrons (pre-equilibrium particles, possible Fermi jets) as a function of all the crystal-ball parameters.

Detector systems of relatively low mass can be put inside the crystal ball, and still cause little loss in the total γ-ray efficiency. Silicon solid-state detectors would be excellent for this purpose, and one or more ΔE-E telescopes consisting of a thin Si transmission or gas-proportional counter and a thick Si detector are obvious choices. Such systems can resolve the Z of product fragments completely up to $Z \sim 50$, and higher values of Z to two or three units. Most experiments on DIC processes have involved such telescopes, and the crystal ball would provide the full gamma-ray information for every event. In such reactions, questions about the amount and alignment of the transferred angular momentum should be relatively easy to answer. The pattern of crystal-ball counters firing should define the plane of the reaction if the γ-ray transitions are mainly stretched E2 (or all dipoles) and there is no twisting motion of the fragments. If there is such motion, it might be possible to determine the alignment of each fragment. Also,

it would be very interesting to study the relationship between kinetic-energy loss and angular momentum transfer throughout the whole range from elastic through quasi-elastic to deep-inelastic collisions. Particle telescopes can also be used to search for high-energy pre-compound charged particles as well as the alpha particles and protons emitted from a compound nucleus, and the γ-ray properties of these processes can then be studied in detail with the crystal ball.

To summarize, we have discussed how the construction of a crystal ball will provide very significant advantages in the study of heavy-ion compound-nuclear events, deep-inelastic collisions, Coulomb excitation, and particle-transfer reactions. There are certainly other areas where such a γ-ray detector will prove useful, as for example, fission studies, the identification and study of isomeric states, and traditional nuclear spectroscopy. In addition, it may be possible to use the crystal ball as energy detectors for high-energy charged particles such as protons, or even electrons or pions. It is clear that such an instrument has the potential to contribute to many areas of nuclear physics studies.

II. DESIGN

A. Physics Capabilities of the Crystal Ball and Their Dependence on Design Parameters

Since the desired quantities to be measured with the crystal ball, such as the γ-ray multiplicity, the total γ-ray energy, or the γ-ray angular distribution, differ in their dependence on the main properties of the crystal ball, e.g., the number of counters and the γ-ray efficiency, we first outline these dependencies.

1. Gamma-ray multiplicity

The response function of the crystal ball for a sharp γ-ray multiplicity completely determines which structures of a multiplicity spectrum can be resolved. Therefore we calculate the probability $P_{Np}(M)$ that p detectors out of a total number of N detectors are triggered, when M photons are emitted from the target. This probability is a function of the following properties of the crystal ball:

a) the number of counters, N

b) the γ-ray efficiency, Ω, of an individual counter

c) the probability, f, for Compton scattering from one counter into its neighbors.

The smaller the total number of counters, N, the higher the probability that two or more γ rays hit the same detector, leading to a reduction in the number of counters triggered and to an increase in the statistical uncertainty of determination. To calculate the probability we make some simplifications by assuming average values of the detector efficiency, Ω, and of the probability of a Compton scattering into neighboring detectors, f. A reduced total efficiency of the system, $N \cdot \Omega$, less than unity results in a

reduction in the number of γ rays detected, and Compton scattering between two counters leads to an increase in the number, as one initial γ quantum may trigger two counters. Both effects results in a larger statistical uncertainty in the number of triggered counters.

The derivation of the probability $\tilde{P}_{Np}(M)$ that p detectors out of N detectors are triggered, when M photons are emitted from the target isotropically <u>without</u> any Compton scattering between counters is given in Ref. 11. An intuitive derivation of $\tilde{P}_{NP}(M)$ is obtained in the following way: The probability not to observe a γ quantum is $(1 - N \cdot \Omega)$ and the probability to observe none out of M quanta is

$$\tilde{P}_{N0}(M) = (1 - N \cdot \Omega)^M \quad .$$

To obtain the probability $\tilde{P}_{N1}(M)$ to observe in one and only one detector at least one γ quantum, we define the quantity $F_x = 1 - (1 - x \cdot \Omega)^M$. F_x is the probability that at least one γ ray is detected in any of x counters out of a total group of M γ rays. The probability that one or more γ rays are observed in one particular detector and none are observed in all other detectors is equal to the probability that at least one γ ray is observed in all N detectors minus the probability that at least one is observed in (N-1) detectors: $F_N - F_{N-1}$. Since there are $\binom{N}{1}$ possible selections of this detector, we obtain

$$\tilde{P}_{N1}(M) = \binom{N}{1}[(1 - (N-1)\cdot\Omega)^M - (1 - N \cdot \Omega)^M] \quad .$$

The probability $\tilde{P}_{N2}(M)$ is found in a similar way from $(F_N - F_{N-2})$ minus the probability that one firing occurs in either one of the two detectors, $2(F_N - F_{N-1})$. This yields $F_N - F_{N-2} - 2(F_N - F_{N-1})$, but there are $\binom{N}{2}$ possible selections of two detectors out of N detectors, so

$$\tilde{P}_{N2}(M) = \binom{N}{2}\left[(1-(N-2)\Omega)^M - 2(1-(N-1)\Omega)^M + (1-N\cdot\Omega)^M\right] .$$

Extending this to p detectors triggered, we obtain

$$\tilde{P}_{Np}(M) = \binom{N}{p}\sum_{n=0}^{p}(-1)^{p+n}\binom{p}{n}\{1-(N-n)\Omega\}^M .$$

In order to generalize the formula of $\tilde{P}_{Np}(M)$ to include Compton scattering, we introduce the probability g_i that i additional γ quanta are produced out of M original ones via Compton scattering out to the first neighboring counters

$$g_i = \binom{M}{i} f^i (1-f)^{M-i}$$

where g_i is a binomial element. For f=0 no additional γ rays are produced; for f=1 each initial γ-ray yields two γ rays.

Now we can decompose the probability $P_{Np}(M)$ with Compton scattering into a sum of probabilities $\tilde{P}_{Np}(M)$ without Compton scattering between detectors by multiplying each element $\tilde{P}_{Np}(M)$ with its probability of occurrence:

$$P_{Np}(M) = \sum_{i=0}^{M}\tilde{P}_{Np}(M+i)\cdot g_i$$

$$= \binom{N}{p}\sum_{i=0}^{M}\sum_{n=0}^{P}(-1)^{n+p}\binom{p}{n}\{1-(N-n)\Omega\}^{M+i}\binom{M}{i}f^i(1-f)^{M-i} .$$

This expression can be transformed into

$$P_{Np}(M) = \binom{N}{p}\sum_{n=0}^{p}(-1)^{n+p}\binom{p}{n}\{1-(N-n)\Omega[1+f(1-(N-n)\Omega)]\}^M .$$

The main properties of the probability $P_{Np}(M)$ are demonstrated in Fig. 1.

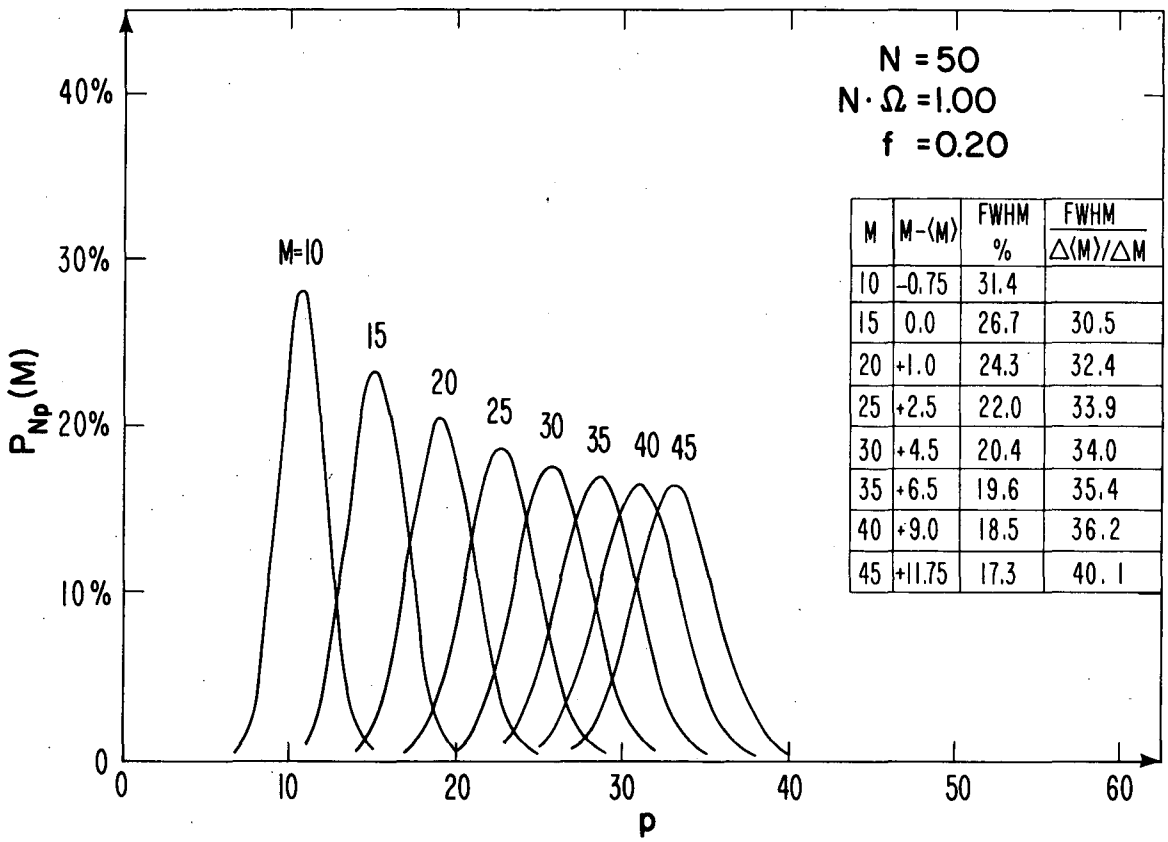

M	M-⟨M⟩	FWHM %	FWHM / Δ⟨M⟩/ΔM
10	-0.75	31.4	
15	0.0	26.7	30.5
20	+1.0	24.3	32.4
25	+2.5	22.0	33.9
30	+4.5	20.4	34.0
35	+6.5	19.6	35.4
40	+9.0	18.5	36.2
45	+11.75	17.3	40.1

XBL 792-317

Fig. 1. Distribution of the number of hits, p, for a spherical shell of 50 counters with 100% efficiency and 20% Compton scattering between crystals.

This shows the probability dependence of the number of hits, p, for multiplicities varying between 10 and 45 in steps of 5 with a fixed number of 50 counters, a 100% efficiency of the total system ($N \cdot \Omega = 1.00$), and 20% Compton scattering between crystals. One obtains rather symmetric bell-shaped response functions. For multiplicities that are low compared to the number of counters, the maximum for the detected folds is higher than the multiplicity originating from the target. For multiplicities comparable to the number of counters, the center position of the fold distribution is lower than the multiplicity originating from the target because of multiple hits in the same counter. There the multiplicity scale becomes strongly nonlinear. As compiled in the table of Fig. 1, the full width half maximum (FWHM) of the bell-shaped curves given as a percentage of the average value, decreases with increasing multiplicity. The increasing overlap of the bell-shaped curves, however, indicates that the resolution decreases for higher multiplicities. We therefore define a new quantity, $FWHM/(\Delta\langle M\rangle/\Delta M)$, as a measure for the multiplicity resolution, dividing the relative FWHM by the nonlinearity of the multiplicity scale. $\Delta\langle M\rangle/\Delta M$ is the ratio between the difference of the measured average multiplicities and the difference of the values taken.

In Fig. 2 the multiplicity resolution is shown for a fixed multiplicity ($M = 30$) as a function of the three determining quantities: the number of counters, N, the total efficiency of the system, $N \cdot \Omega$, and the probability, f, of Compton scattering from the central counter into its neighbors. As a function of counter number, we find a very strong dependence for $N \leq 2 \cdot M$. Above about 250 counters the improvement of the resolution with counter number is relatively small, and not very significant compared to the influence of the other factors.

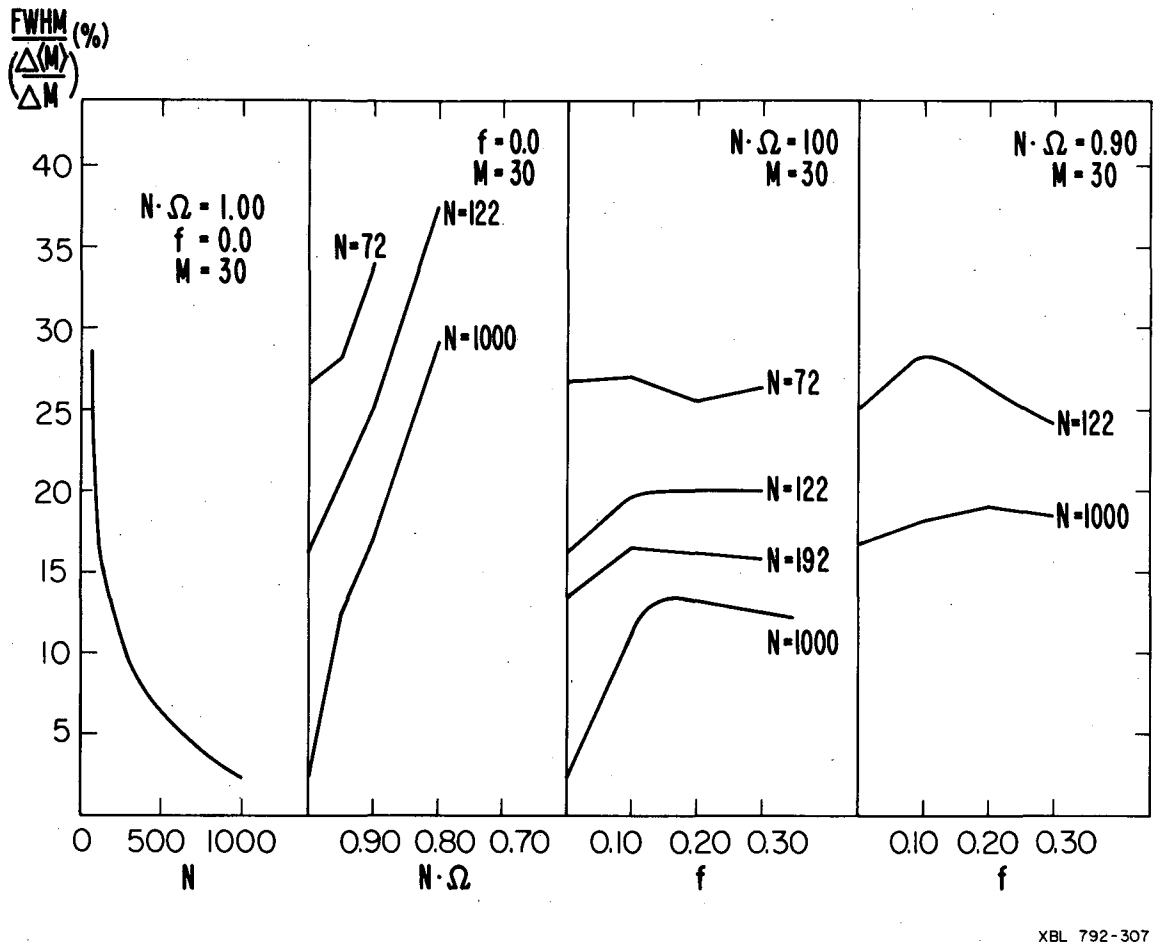

Fig. 2. The multiplicity resolution (the FWHM in percent divided by $\Delta\langle M\rangle/\Delta M$, the ratio between the difference of the measured average multiplicity and the original differences) as a function of the number of counters, N, the total efficiency $N\cdot\Omega$, and the probability for Compton scattering between one crystal and its neighbors, f.

One observes a rather strong dependence on the total efficiency. And as a function of Compton scattering, there is only a little change in resolution after an initial rise. A significant shift in the average value <M> as a function of f remains. The γ-ray energy dependence of the factor f therefore will lead to an additional broadening, which can be corrected to first order on an event-by-event basis using the measured γ-ray energies. For a system with 162 counters, a total efficiency of 90% and a Compton scattering from one crystal into its neighbors between 20% and 30%, a multiplicity resolution of about 20% will be obtained. The response functions for such a system are shown in Fig. 3.

2. Total gamma-ray energy

For the measurement of the total γ-ray energy the subdivision into individual counters and their Compton scattering is of no relevance. The total energy resolution is mainly determined by the total efficiency $\varepsilon = N \cdot \Omega$ of the system.

We make the simplifying assumptions that we have a fixed number, M, of γ-rays, all with the same energy $\bar{E}_\gamma$, which are detected with a probability ε for the full photoenergy peak and 0 otherwise. Thus $(1-\varepsilon)$ is the probability that a γ-ray is not detected at all. (The formalism can be, and has been, extended to include a Compton contribution, but this makes no significant difference in the conclusions.) Then the response function of the system for the original energy $E_\Sigma = M \cdot \bar{E}_\gamma$ is given by:

$$P(K) = \binom{M}{K} \varepsilon^K (1-\varepsilon)^{M-K}$$

measuring the energy in units of $\bar{E}_\gamma$.

The average detected energy $\bar{E}$ is given by

$$\bar{E} = \bar{E}_\gamma \cdot \sum_{K=0}^{M} K \cdot P(K) = \varepsilon \cdot M \cdot \bar{E}_\gamma = \varepsilon \cdot E_\Sigma \quad .$$

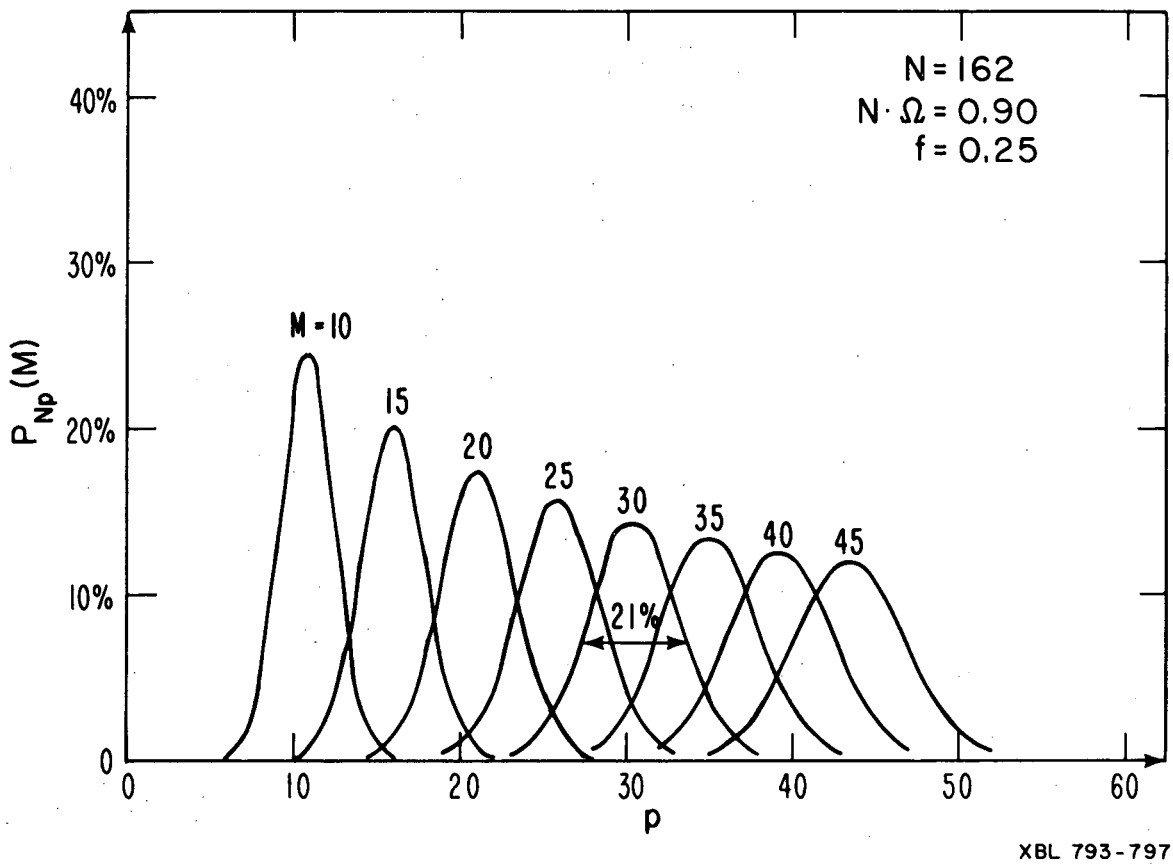

Fig. 3. Distribution of the number of hits, p, for a spherical shell of 162 counters with 90% efficiency and 25% Compton scattering.

For the variance of the distribution σ we obtain:

$$\sigma^2 = \bar{E}_\gamma^2 \sum_{K=0}^{M} (K-M\cdot\varepsilon)^2 \cdot P(K) = \bar{E}_\gamma^2 \cdot M\cdot\varepsilon(1-\varepsilon) = \bar{E}\cdot\bar{E}_\gamma(1-\varepsilon) \quad .$$

When determining the series of K, we used the three relations:

$$\sum_{K=0}^{M} P(K) = 1 \; ; \qquad \frac{d}{d\varepsilon}\sum_{K=0}^{M} P(K) = 0 \; ; \qquad \frac{d^2}{d\varepsilon^2}\sum_{K=0}^{M} P(K) = 0 \; .$$

For a photopeak efficiency of $\varepsilon = 0.80$, a total γ-ray energy $E_\Sigma = 30$ MeV, and an average γ-ray energy $\bar{E}_\gamma = 1.0$ MeV, we obtain a FWHM = $2.35 \cdot \sigma$ = 5.2 MeV. The FWHM measured with respect to the mean detected energy is 21%. Since the expected resolution of an individual counter is about 7% for 1 MeV γ rays, and decreases with increasing energy, the total energy resolution is predominantly determined by the total efficiency of the system. While this efficiency, ε, refers to the detected fraction of the total γ-ray energy, the system has a larger efficiency with respect to the multiplicity measurement, since only the triggering of a counter is demanded there.

3. Gamma-ray angular distributions

Let us assume that the γ rays are emitted by a completely aligned nucleus with large angular momentum I. The expression[15] for the angular distribution of stretched E2 transitions is, $W(\theta) = 5/4(1 - \cos^4\theta)$, and for stretched dipole transitions, $W(\theta) = 3/4(1 + \cos^2\theta)$, where θ is the angle of emission of the γ-quanta measured with respect to the angular momentum axis. For compound nuclear reactions, the very marked minimum in the E2 angular distribution allows a rather precise determination of

the spin direction within the plane normal to the beam axis via the known E2 transitions of the yrast bump. The multipolarity and type of transition for other γ-ray energies may then be determined by comparison with the E2 behavior. Compared to an isotropic distribution, the intensity of stretched E2 transitions is enhanced by 23% within the equatorial band from $60° \leq \theta \leq 120°$, corresponding to one-half the surface of the sphere. This leads to an enhanced pile-up compared to the estimates assuming an isotropic distribution. While the Compton scattering into neighboring crystals does not distort the angular distribution on the average, the pile-up reduces deviations from an isotropic distribution. The study of angular distributions therefore favors the selection of larger counter numbers even at the expense of increased Compton scattering.

4. Energies of individual gamma-ray transitions

The spectra of individual counters are distorted by pile-up and Compton scattering. However, each crystal with its surrounding elements may be regarded as an anti-Compton spectrometer. The average number of counters, n, which had only a single hit and for which no hits occurred in neighboring detectors is given by

$$n = (1-f)MN\Omega(1-\Omega)^{(M-1)}(1-L\Omega)^{(M-1)(1+f/2)}$$

where Ω is the efficiency of the individual counters, N the total number of counters, L the number of neighboring counters, M the γ-ray multiplicity originating from the target, and f the probability of Compton scattering into neighboring counters. The factor $MN\Omega(1-\Omega)^{M-1}$ corresponds to the probability that one and only one γ ray hits the central counter, and the factor (1-f) excludes those that Compton scatter into surrounding counters. The factor $(1-L\Omega)^{(M-1)(1+f/2)}$ represents the further decrease

from γ rays that hit counters in the first circle or Compton scatter into the first ones around the central counter. In Fig. 4 this average number of anti-Compton counters, n, is shown as a function of counter number N for f = 0.20; L=6; M=30, and Ω = 0.90/N. The probability p for pile-up in a counter with the anti-Compton requirement is:

$$p = \frac{1-(1-\Omega)^{M(1-f)} - M(1-f)\Omega(1-\Omega)^{M-1}}{1-(1-\Omega)^{M(1-f)}}$$

For 162 counters, a γ-ray multiplicity of M=30, f=0.2, and an efficiency Ω = 0.90/162, about 9.4% pile-up occurs. This does lead to some degree of uncertainty in the determination of γ-ray energies on an event-by-event basis (although, on the average, energy spectra can be corrected for pile-up in the unfolding procedure).

However, since there are several anti-Compton counters with a good energy-response function for a single event, it is possible to derive energy-correlated quantities for the continuum γ rays on an event-by-event mode, remembering the error introduced by pile-up. For example, let us assume that all transitions in the yrast bump are rotational with energies given by $E = (4I - 2)\hbar^2/2\theta$, where I is the spin of the upper state and there is a fixed moment of inertia, θ. In a spectrum of E_2-E_1, the difference in energies between two coincident (anti-Compton) γ-ray counters, there will be a minimum at the origin, and a sequence of peaks on each side spaced at $8\hbar^2/2\theta$. With a small spread in the initial moments of

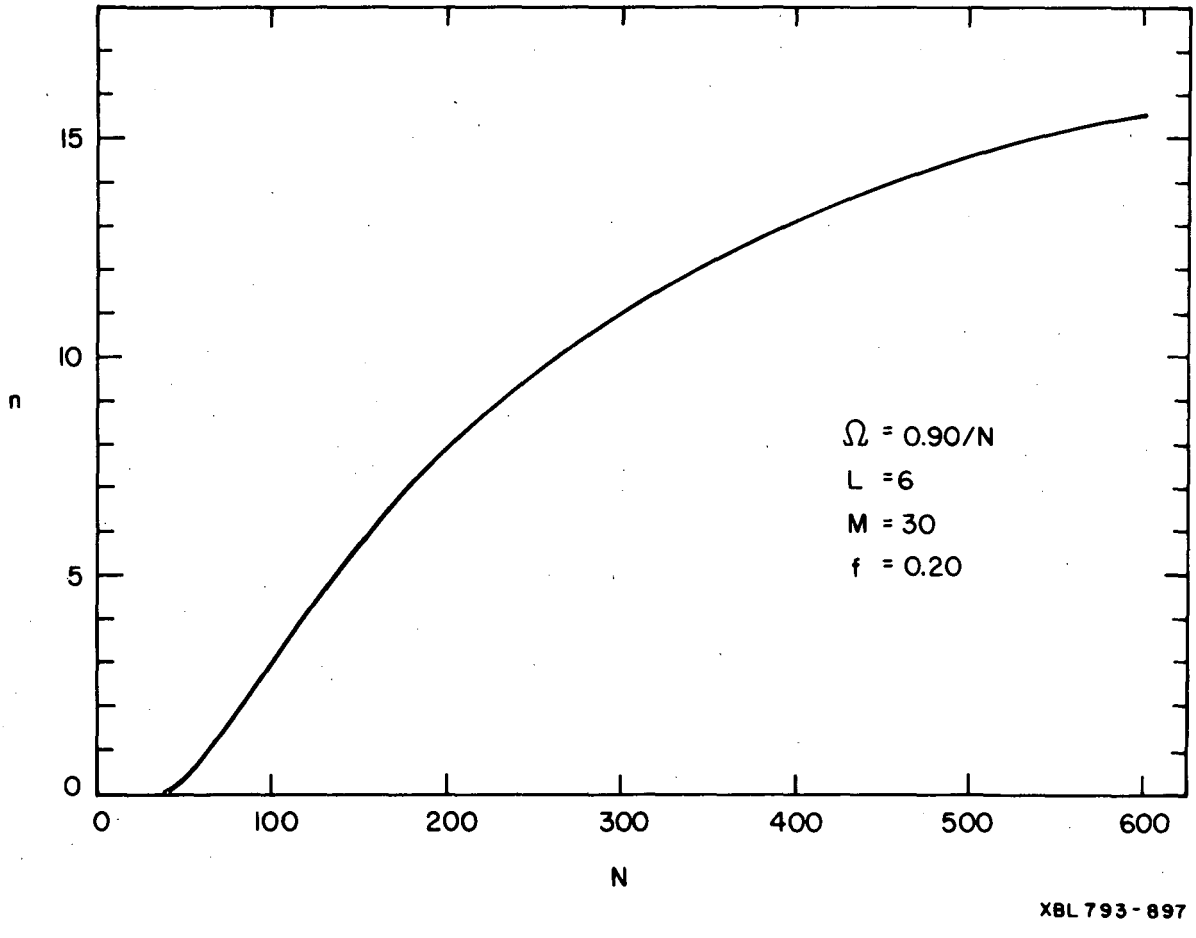

Fig. 4. The number of counters, n, without pile-up and no neighbor counters firing as a function of the total number of counters, N, with a total efficiency of 90%, a multiplicity of 30, f = 0.2, and six nearest neighbors for each crystal.

inertia, these peaks will gradually spread in width and decrease in heighth in proportion to their distance from the origin. The study of these structures (to determine the magnitude and spread of the moments of inertia) requires a resolution in the detectors of the order of $8\hbar^2/2\theta$, and the most important region of the spectrum is that between consecutive transitions. Statistics for this region increase very rapidly with the number of anti-Compton type counters. The increase of n with counter number N of Fig. 4 suggests selecting a counter number, N, as large as possible, but the method still seems feasible for 122 counters. A comparison of the energy resolution with predicted energy differences between rotational transitions shows that a rather good energy resolution for the NaI counters is required. It will, in fact, determine up to which mass number these studies can be performed.

5. Neutron gamma-ray separation

The large volume of the crystal ball leads to a large fraction of events where neutron capture or inelastic neutron scattering in the NaI crystal distorts the measured γ-ray multiplicity, total energy, and angular distribution. The disturbance by neutron capture becomes especially important for the most interesting but rare events with rather high total energy, since the capture process leads to a large amount of γ-ray energy (7-8 MeV), which can be in coincidence with the more numerous low total-energy events, and so falsely give too high a proportion of high-energy events. Taking a capture cross section[16] of 80 mb for ^{127}I and 1 MeV neutrons, a crystal ball with a shell thickness of 6 inches will detect a neutron capture in about 8% of all events for a (HI,4n)-reaction. The rather isotropic scattering of neutrons within

the crystal will lead to a further increase of the fraction of events with neutron capture. A free scattering length of λ = 5.3 inches for neutrons is obtained from a scattering cross section[16] of about 5 b. The inelastic neutron scattering cross section[16] of about 2 b for ^{127}I results in about two inelastically scattered neutrons per event with an average γ-ray energy release of about 400 keV per neutron.

We want to discriminate neutrons from γ rays by the difference in flight time from target to the NaI shell. With achievable time resolutions by NaI detectors of FWHM = 2-3 ns, a separation seems possible if the inner radius of the NaI shell is of order 23 cm or larger. Such a *lower limit for the inner radius of the NaI shell* represents an important restriction for the design. In addition, neutron-capture events possibly may be identified by the rather large energy which is deposited in a single crystal. Both methods of discriminating neutrons from γ rays will be tested with a prototype sector of the crystal ball.

B. Determination of Specific Design Parameters

The preceding discussion of the different properties of the crystal ball now allows a rather simple specification of the main design parameters. These are:

a) the total number of counters

b) the size of an individual counter

c) the shape of the total system.

1. The number of counters

The γ-ray multiplicity resolution is one of the important figures of merit of the crystal ball. For a given multiplicity, M, this multiplicity

resolution of a system with N counters is a rapidly deteriorating function of decreasing counter number N in the region $N < 2M$ (compare Fig. 2). Using the relation $N > 2M$, the minimum number, N_{min}, is determined by the maximum number of γ rays expected in a nuclear event. For larger nuclear spins the average multiplicity of emitted γ rays is about half the average angular momentum of good rotational nuclei. Maximum spin values of about 70 $\hbar$ are predicted for nuclei with mass numbers of about 120. The spin is limited by either fission or alpha-particle emission.[17] This leads to an estimated upper multiplicity of about 35-40 for compound nucleus reactions. In deep-inelastic reactions involving two final nuclei with about equal masses of 160, γ-ray multiplicities up to 45 have been observed and somewhat larger values might be expected. Deep inelastic reactions followed by sequential fission should not lead to higher multiplicities since a large part of the spin of the original nucleus is transferred into orbital angular momentum of the fragments. Assuming therefore a maximum multiplicity of 50, we obtain a lower limit for the counter number of $N_{min} \approx 100$. If one also assumes the multiplicity resolution as a basic criterion for determining the maximum number of counters, an investigation of the multiplicity resolution shows that beyond 250 counters other factors like the total efficiency become dominant and little improvement is obtained by increasing the counter number. Therefore

$$\boxed{100 < N < 250} \quad .$$

Geometrical considerations on the tiling of a sphere with hexagons and pentagons (see section II.B.3) lead only to six configurations within these limits: with 122, 132, 162, 192, 212, and 252 counters. Further

symmetry considerations favor the solutions with 122, 162, and 252 elements. Since the production of the counters, the electronics and also the price of the support frame are a roughly linear function of the counter number, the price of these systems can be predicted by scaling the price for 162 elements with the counter numbers. Though many arguments, e.g., the number of anti-Compton counters, the study of the γ-ray angular distribution, etc., favor large counter numbers, we must come to a compromise with the cost, and have tentatively chosen a configuration with 162 elements. Our proposed testing of a module with six counters will either confirm this decision or suggest a different number.

2. Size of the individual counters

The strong dependence of the multiplicity resolution on the absolute efficiency (see Fig. 2) leads to the requirement that at least 90% of all γ rays should be detected. In Fig. 5 the three dashed curves show the fraction of γ rays which pass through a NaI shell of 10, 15, and 20 cm thickness without any interaction. The calculation is based on published total absorption coefficients.[15] If the detector is triggered only by events where more than 100 keV of energy are deposited in the crystal, the absorption cross section due to Compton scattering is decreased by less than 10%. This can be seen from the differential Compton cross section[15] as a function of the energy of the scattered electron. The three curves of Fig. 5 show, therefore, that a shell of 15 cm thickness seems to be sufficient. The real total efficiency of the system will be about 3% smaller since the material of the cans and the light reflecting material surrounding each crystal has a thickness of about 1 mm. These

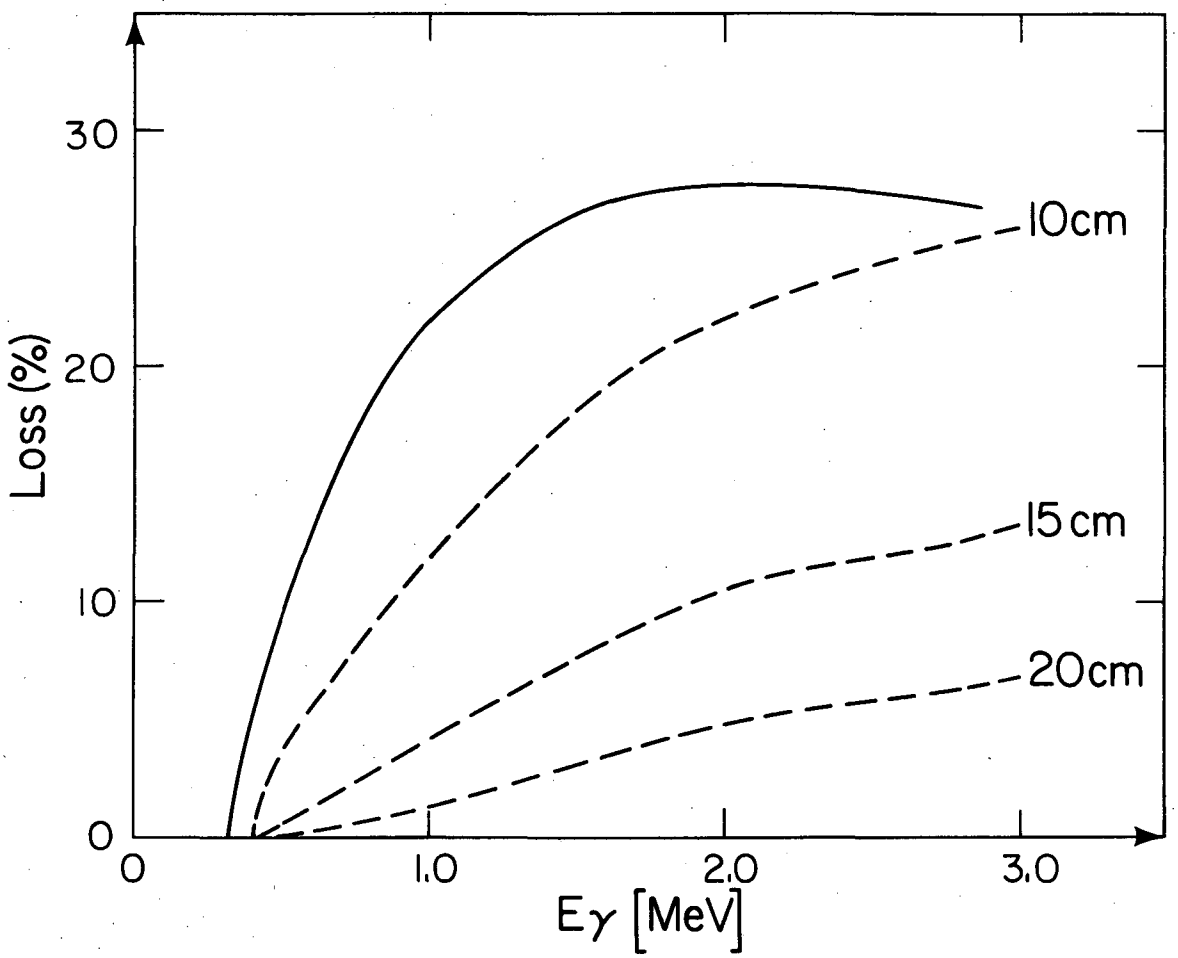

XBL 792-320

Fig. 5. Fraction of the γ rays which pass through a NaI shell of 10, 15, and 20 cm without any interaction (dashed lines). Fraction of γ-ray energy not detected, assuming one Compton scattering only, for 15 cm shell (full line).

theoretical estimates indicate that with 15 cm long crystals one obtains a total average efficiency of about 90% for the measurement of the multiplicity. This number will be determined more accurately with a test module.

With respect to the total γ-ray energy detected, the efficiency is smaller and can to a certain extent be estimated by using the true absorption coefficient.[15] There the Compton cross section is weighted with the fraction of the energy transferred to the electron. The full curve in Fig. 5 shows this loss in detected energy for a 15 cm thick NaI shell as a function of γ-ray energy. The actual total-energy efficiency of the crystal ball depends on the degree of absorption of the scattered γ rays and will be better than the prediction.

In a measurement with a 33×20 cm NaI sum spectrometer with the source placed in the center, a total loss of energy of 19% was obtained for 1.17 MeV γ rays. Therefore an efficiency around 80% with respect to the detected total energy is expected. Again, more accurate efficiencies will be obtained with the test module.

After specifying the *length of each individual crystal to be about 15 cm*, we have to consider the shape and diameter of each crystal. It is immediately clear that the radial cross section of each crystal should be as close to a circle as possible to minimize the Compton scattering from one crystal into neighboring ones for a given NaI volume. In our design we have cross sections of rather regular hexagons or pentagons. For the calculation of the properties of the crystal ball we need the percentage of Compton scattering, f, from one crystal into its neighbors. This depends on the average diameter of the crystal and on the γ-ray energy. Though there are many publications on the peak-to-Compton ratio for

different crystal shapes, the strong angular dependence of the Compton scattering makes it difficult to derive from those values what fraction is scattered to the lateral sides compared to the end faces. We therefore performed a measurement with two 14 cm long crystals which have a U-shaped cross section. Both crystals touch each other along their 14 cm by 7.6 cm surfaces. From this measurement we obtained an estimate for the fraction, f, of Compton scattering through all lateral sides. This estimated fraction is shown in Fig. 6 as a function of γ-ray energy. The fraction, f, shows a γ-ray energy dependence much like the Compton-to-total ratio. For an average γ-ray energy of 1 MeV we obtain $f = 0.2$, which is within the range of values used in earlier estimates. The exact values of f as a function of gamma-ray energy will be obtained with the test modules. Since the absorption length of a 1 MeV γ ray in NaI is 4.7 cm, the fraction of Compton-scattered quanta which leave the central crystal goes as $\exp[-\alpha d\mu]$, where d is the average diameter of the crystal cross section, μ is the absorption coefficient for 1 MeV γ-quanta in NaI, and the constant α takes care of the averaging over scattering angles and over the position where the scattering takes place. Empirically, α has a value of 0.8 for a 14 cm by 7.6 cm crystal. Therefore a first-order estimate of the dependence of f on the average diameter d is

$$f = f_0 \, e^{-(d-d_0)\cdot\alpha\cdot\mu} \quad .$$

This suggests that f does not change significantly within reasonable limits for the average diameter. On the other hand, the diameter of a crystal should be larger than about 3 cm, because otherwise Compton scattering into second-nearest neighbors also becomes important.

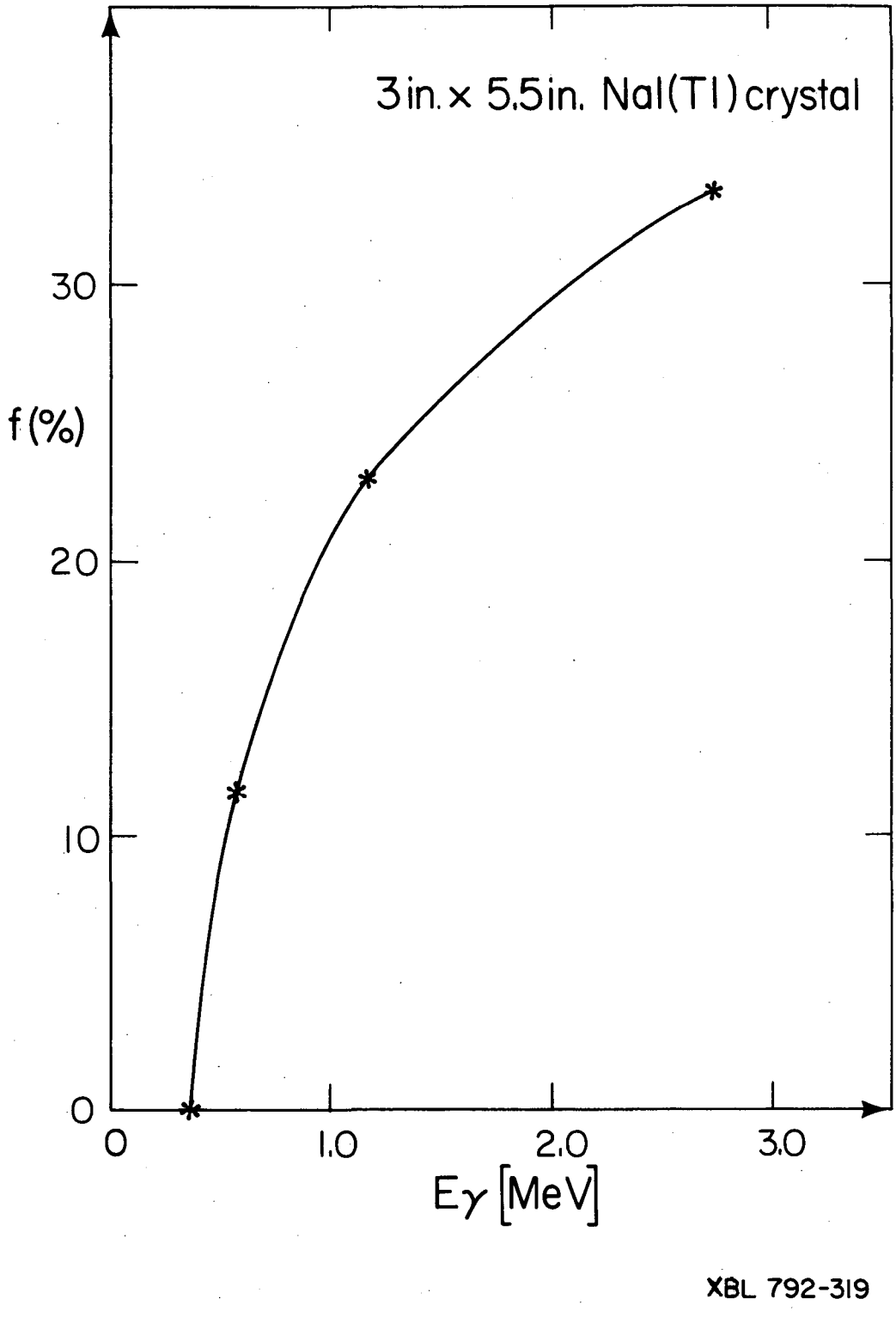

Fig. 6. Fraction of γ rays scattering into all neighboring crystals as a function of γ-ray energy for a 14 cm long, 7.6 cm diameter NaI crystal.

If one wants to keep the smallest crystal diameter no less than 7 cm, the number of crystals immediately leads to another lower limit for the inner radius of the crystal shell, namely, 23 cm for 162 elements.

3. Shape of the total system

The individual elements of the crystal ball consist of tapered prisms, which if extended would meet in the center of the sphere. Therefore we only have to specify the inner (or outer) faces of the prisms, and the search for the optimum shape of the crystal ball reduces to the question, "how to tile a sphere in an optimum way with polygons, but without gaps or overlaps?" That is, how to find the optimum polyhedron. For an introduction to the following discussion we recommend the book, Polyhedra, A Visual Approach," by Anthony Pugh.[18)]

We now list some requirements which will allow us to select the optimum shape:

1. *All polygons of the polyhedron should cover the same solid angle.* This requirement allows the determination of gamma-ray multiplicities from the number of counters firing, without specifying the individual counters.

2. *The ratio between circumference and the area of the polygons should be as small as reasonably possible.* This leads to the minimum Compton scattering between crystals for a given volume of the crystals. The more polygons meet at a vertex of the polyhedron the sharper (in general) the angle of the polygons and the larger the scattering from one crystal into others. We therefore introduce the further requirement:

3. *At each vertex of the polyhedron only three polygons should meet.*

4. *The number of different polygons should be as small as possible.* This simplifies the construction, production, assembly and replacement of defective counters. Later we add for the same reason that the polyhedron should have a high degree of symmetry.

5. *The number of faces of the polyhedra should be larger than 100.* This requirement was obtained from the discussion earlier of the number of counters.

From these requirements rather general properties of the desired polyhedra can be derived.

In Ref. 18 one finds a compilation of all regular polyhedra; they consist of:

1. The five Platonic polyhedra, where at each vertex the same number of a particular type of regular polygon meet (tetrahedron, octahedron, cube, icosahedron, and dodecahedron).

2. The thirteen Archemedian polyhedra and prisms, in which the base is a regular n-gon while the lateral faces are squares, and the so-called skew prisms, in which the base is a regular n-gon while the lateral faces are 2n equilateral triangles. This second class of polyhedra again consist of regular polyhedra in which at every vertex the same number of polygons meet, but now they may be of different types.

3. 92 convex polyhedra, which represent the group where dissimilar arrangements of regular polygons occur about each of the vertices.

A scan of all these polyhedra shows that in most cases the polygons do not cover the same solid angle. If they do, the number of faces is much smaller

than 100, and in many cases some polygons are triangles, which is undesirable because of the large ratio between circumference and area. Therefore the desired polyhedra belong to the much more general but less investigated class of polyhedra with at least one type of *non-regular polygon*.

We now want to show that the class of optimal polyhedra always has 12 pentagons and a variable number of hexagons.

Our requirement that at each vertex only three polygons meet, leads to strong restrictions on the possible solutions. Let us assume that we have a polyhedron consisting of N_6 hexagons (regular or non-regular) and N_x x-gons (regular or non-regular), in which at each vertex three faces meet. We now prove that such a polyhedron has to have, besides hexagons, either 12 pentagons or 6 squares or 4 triangles. We introduce in each polygon of the polyhedron a center point and connect it with the vertices of the polygon. Then the polyhedron becomes a network of triangles. There are $6 \cdot N_6 + x \cdot N_x$ triangles, and the sum of all face angles is $180° \ (6 \cdot N_6 + x \cdot N_x)$. Since each triangle has three vertices and six triangles meet at each vertex (except for that one in the center of each polygon which has x triangles meeting), the number of vertices, V, is: $V = (6 \cdot N_6)(2/6 + 1/6) + (x \cdot N_x)(2/6 + 1/x)$. For any convex polyhedron[18] the sum of all face angles is given by

$$360°V - 720°$$

if V is the number of vertices. Therefore we obtain

$$180° \cdot (6 \cdot N_6 + x \cdot N_x) = 360° \left[(6 \cdot N_6) \cdot \left(\frac{3}{6}\right) + (x \cdot N_x)\left(\frac{2}{6} + \frac{1}{x}\right)\right] - 720° ,$$

or

$$N_x = \frac{4}{2 - \frac{x}{3}} .$$

For $x = 6$, N_x is infinite, corresponding to the tiling of the infinite plane with hexagons. For $x \geqslant 6$ no solutions exist. By setting x equal to 5, 4, and 3, we obtain that the polyhedron contains either 12 pentagons or 6 squares or 4 triangles respectively. If one would introduce polygons with more than 6 edges one would have to introduce an additional number of polygons with less than 6 edges to obtain the correct sum of all face angles.

The larger the number of faces of a polygon, the smaller the average length of a side for a given area. Polygons with different numbers of edges but equal area bordering each other will, in general, deviate the more from a regular shape, the bigger the difference in the number of edges. The demand for an optimum ratio of circumference to area for all polygons, on the average, therefore, leads to an optimum solution of polyhedra with hexagons and 12 pentagons. Hexagons combined with squares or triangles lead to hexagons strongly deviating from regular ones, when they neighbor the squares or triangles. Polygons with more than 6 edges increase the number of different polygons of the polyhedron and also lead to more polygons with edges less than 6, which have unfavorable circumference to area ratios. So we obtain an optimum solution of hexagons combined with 12 pentagons without specifying which polygons are regular and without specifying their arrangement.

We now introduce an additional requirement for a high degree of symmetry of the polyhedra, demanding that the center of each pentagon be a five-fold symmetry axis of the polyhedron. Other solutions with randomly oriented irregular hexagons and pentagons are possible, but the calculation of such figures will be complex, and since the shapes are irregular, the difficulties of production will be much greater.

In Fig. 7 polyhedra containing hexagons and 12 pentagons, with each pentagon representing a five-fold symmetry axis, are shown as a function of increasing number of faces. All these polyhedra have the symmetry properties of the dodecahedron — the first polyhedron of Fig. 7 and its dual, the icosahedron. Connecting the centers of the pentagons by straight lines one obtains the icosahedron; connecting the mid-points of the connections between neighboring pentagon centers one obtains the dodecahedron. In Fig. 8 we show the icosahedron and dodecahedron viewed from their face, edge, and vertex.

One can characterize these polyhedra by two 5-fold symmetry axes; the operation of the first 5-fold symmetry axis on the other 5-fold axis leads in total to 12 points around which one has a 5-fold symmetry — the centers of the 12 pentagons.

The strange sequence of the number of faces of these polyhedra, i.e., 12, 32, 42, 72, asks for an explanation, and one wants to know all possible solutions. We introduce with Fig. 9 a complete ordering scheme for all possible solutions. There one pentagon is plotted at the tip of a triangle built up from a mesh of hexagons. If one replaces a particular hexagon by a pentagon, the demand for the 5-fold symmetry with respect to the center of the pentagon immediately determines the position of the third pentagon. The center points of the three pentagons form an equilateral triangle of the basic icosahedron, and thus the total polyhedron is defined. At each side of the hexagons the number of faces of the corresponding total polyhedron is written. By comparing Fig. 9 and Fig. 7 one can easily identify some configurations. For the radial sides of the hexagons no numbers are given, since the pentagon will touch another edge, which is closer to the original pentagon at the tip. Because of

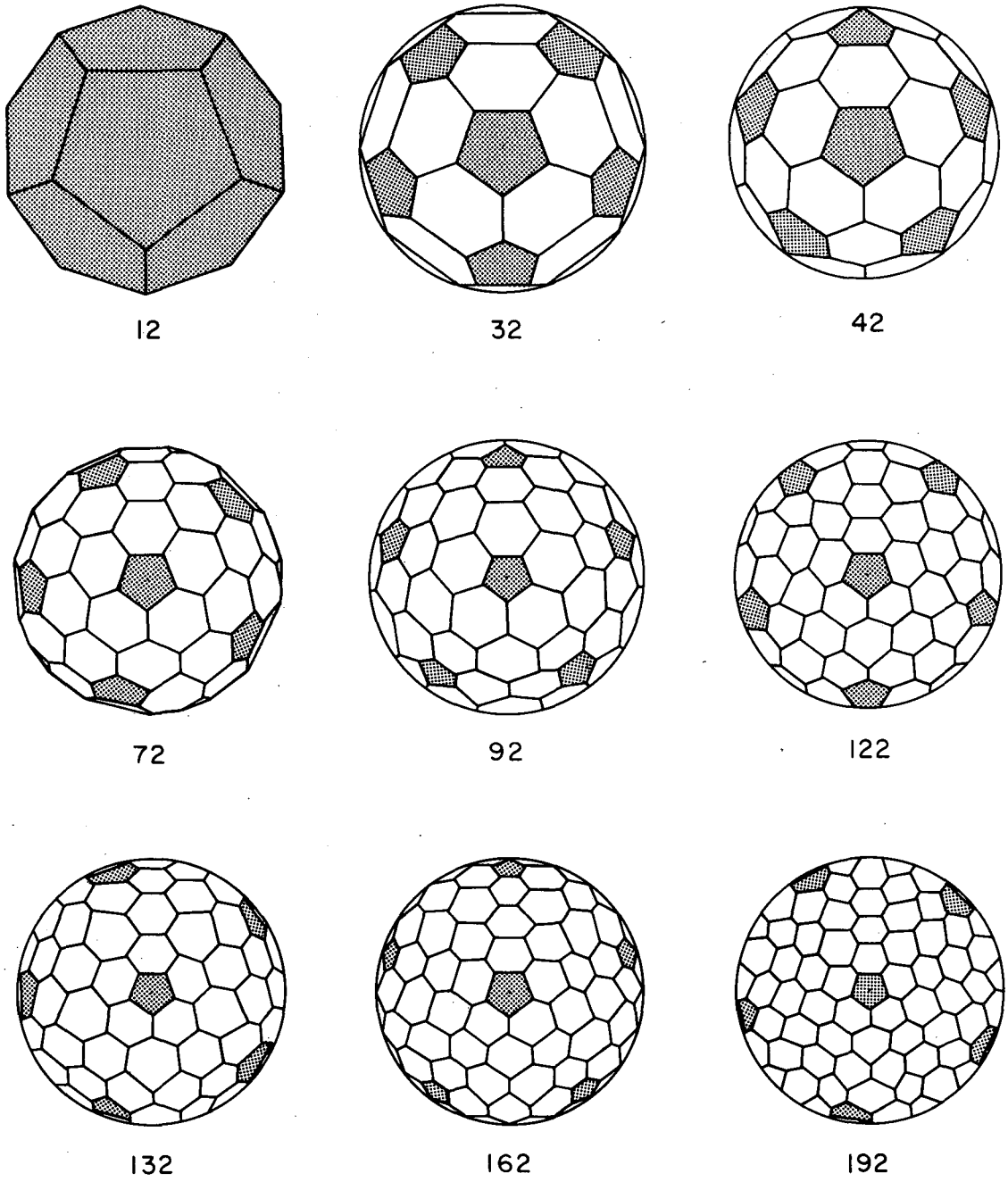

Fig. 7. Polyhedra containing 12 pentagons and hexagons

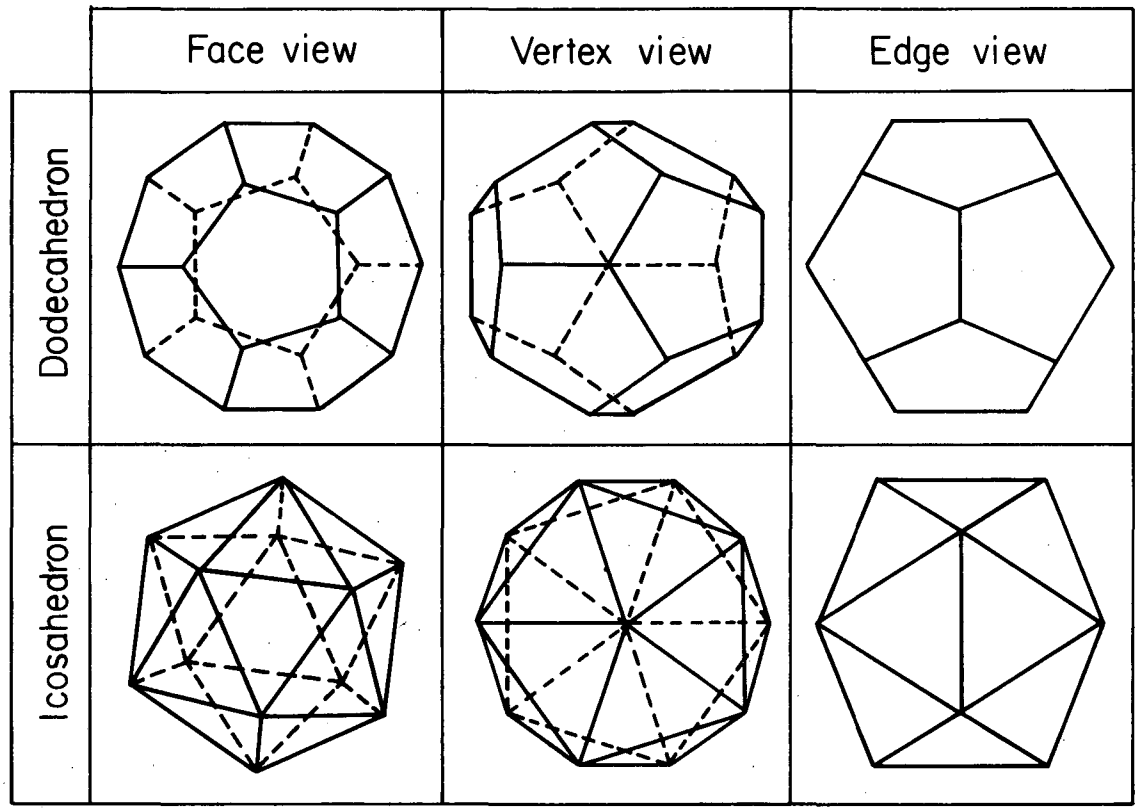

XBL 792-312

Fig. 8. Face, vertex, and edge view of a dodecahedron and an icosahedron.

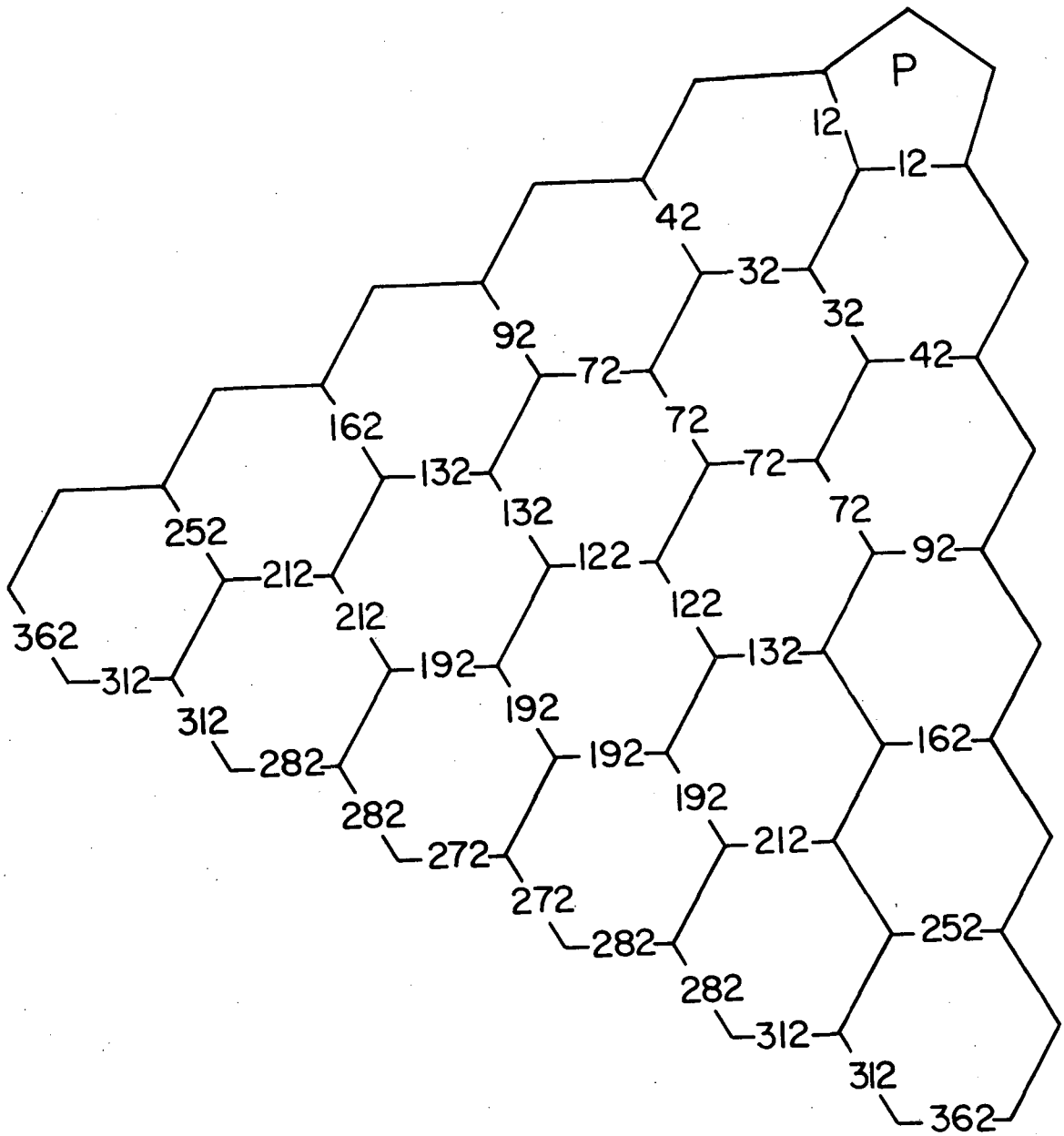

XBL 792-313

Fig. 9. Ordering scheme to derive configurations based on 12 pentagons and varying numbers of hexagons (see text, section II.B.3).

the five-fold symmetry, only hexagons in a sector of 60° have to be considered. Every possible arrangement of hexagons around a pentagon is covered in this scheme, which therefore allows an ordering of all these polyhedra.

The number, N, of faces of these polyhedra is given by:

$$N = 10 \cdot (h^2 + k^2 + h \cdot k) + 2$$

with integer values (0,1,2,...) for h and k. This allows an immediate prediction of all possible numbers of faces.

The first few numbers in this sequence are: 12, 32, 42, 72, 92, 122, 132, 162, 192, 212, and 252.

To decide which of the six solutions in the region of 100 to 250 counters: 122, 132, 162, 192, 212, and 252 is best, we have to study their properties, including their symmetry properties. The latter are mainly determined by the properties of the basic icosahedron and dodecahedron (see Fig. 8).

There are always two pentagons opposite each other with respect to the center of the polyhedron (but are rotated 36° against each other). If a hexagon occurs in the center of a triangular face (for example in the solutions with 32, 92, 122 faces), another hexagon occurs in the opposite face, that is, at 180° with respect to the center of the polyhedron. This is apparent from the face view of the icosahedron in Fig. 8. If there are hexagons in the middle of the connecting lines between the centers of neighboring pentagons (solutions with 122, 162, 252 faces) they have the property that there are equivalent hexagons at 90° with respect to the center of the polyhedron. This can be deduced from the edge-view of the icosahedron of Fig. 8. If those hexagons are used as portholes

of the crystal ball, one has a hole to bring the beam in and out, and holes at 90° up and down and left and right of the center. Studies at 0° and 90°, where counters of the crystal ball are replaced by other types of counters, are of considerable value as these are usually extrema of angular distributions. Furthermore, ten of those hexagons lie in the equatorial plane with respect to two opposing pentagons with a constant angle of 36° between them.

These properties of the center points of the edges of the icosahedron make the selection of polyhedra with 122 and 162 faces more desirable. Both consist of four basic types of polygons. Since both configurations seem equivalent, other considerations, such as the difference in price compared to the gain in resolution of the measured quantities, must be taken into account to choose one or the other of these systems.

Some arbitrariness exists in the actual determination of the shapes of the crystals, because one has to select which hexagons are regular or not. The hexagons neighboring the pentagons cannot be regular, since they have one side in common with the pentagon and have to cover the same solid angle. In the case of the 122-element configuration, we selected the hexagon in the center of the triangle of the basic icosahedron to be regular because the selection of the hexagons on the lines connecting the pentagons led to more strongly distorted hexagons neighboring the pentagons. In the case of the 162-element system, on the other hand, we selected the hexagon on this connecting line to be regular since the deviations from regularity for the other hexagons are not very large and it seems most suitable to have regular hexagons as units which may be used as portholes for the system. After selecting these hexagons as regular ones, the shapes

of the other hexagons are immediately fixed by the requirement of equal solid angles for all the polygons and the 120° symmetry of the triangle between the neighboring pentagons.

In Tables 1 and 2 we specify the arc lengths between the vertices of the polyhedra on the sphere. In the case with 122 elements the sides of the triangular faces of the basic icosahedron are divided into six parts, and the representation[18] is called a six-frequency icosahedron. In the system with 162 elements we start with a dodecahedron in which each pentagonal face is divided into five equal triangles. The sides of each of these triangles is further divided into four parts, and the representation is called a four-frequency dodecahedron.

One could imagine obtaining a polyhedron by connecting the vertices of the polygons on the sphere with straight lines. But then one faces the problem that the six vertices of a non-regular hexagon lying on a sphere do not lie in a common plane. (In our case these deviations are small, since the deviations from a regular hexagon are small.) Therefore the vertices on the sphere and their connecting lines are used only to specify the radial faces of the crystals. This representation on the sphere made the determination of equal solid angles for the different polygonal crystals easy.

The actual crystals have flat (parallel) front and end faces. The shapes of these faces are given for a sphere with a unit radius in Tables 3 and 4. They were obtained by introducing tangential planes normal to the radius through the center points of each polygon and then projecting the arcs on the sphere (from its origin) on to those planes. As a result, neighboring polygons do not, in general, meet

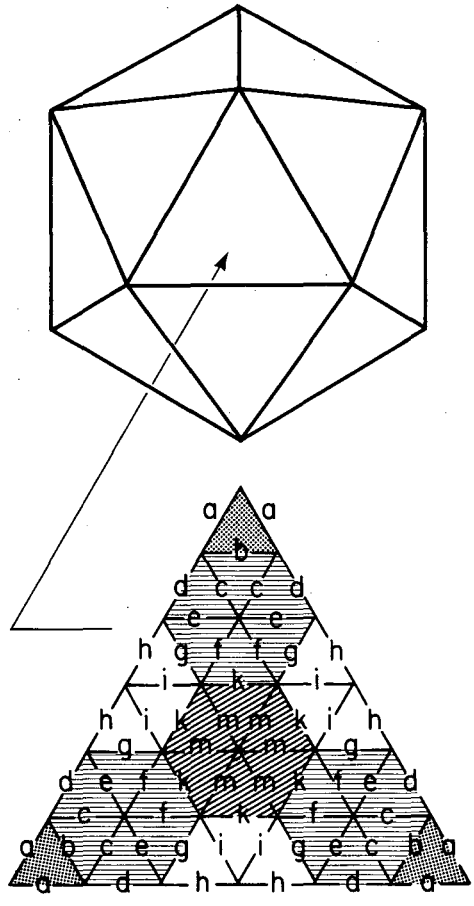

XBL 792-308

a = 0.207741
b = 0.243059
c = 0.190807
d = 0.176757
e = 0.222301
f = 0.190582
g = 0.202734
h = 0.169066
i = 0.215728
k = 0.197976
m = 0.198952

TABLE 1. Arc lengths for a six-frequency icosahedron, dividing the sphere into 110 hexagons and 12 pentagons of equal area.

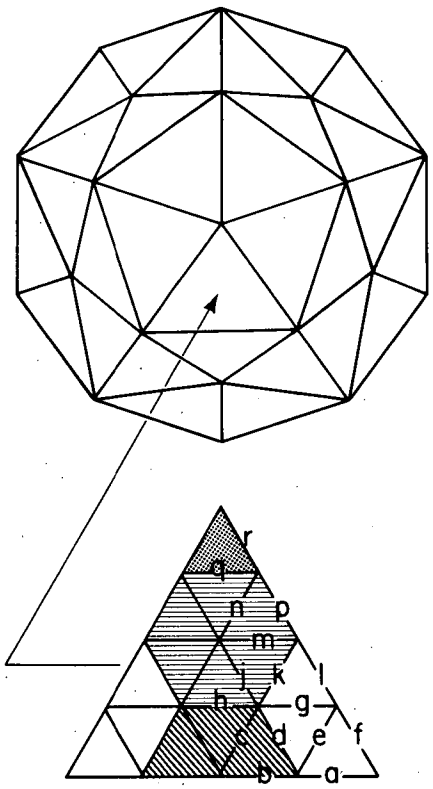

XBL 792-311

a = 0.192179

b = 0.172685

c = 0.172685

d = 0.172040

e = 0.174179

f = 0.149429

g = 0.201765

h = 0.172040

j = 0.142340

k = 0.163529

ℓ = 0.149429

m = 0.204913

n = 0.178088

p = 0.173138

q = 0.211274

r = 0.180363

TABLE 2. Arc lengths for a four-frequency dodecahedron, dividing the sphere into 150 hexagons and 12 pentagons of equal area.

TABLE 3. Length of hexagons and pentagons of a polyhedron with 122 elements, having an inscribed touching sphere of unity.

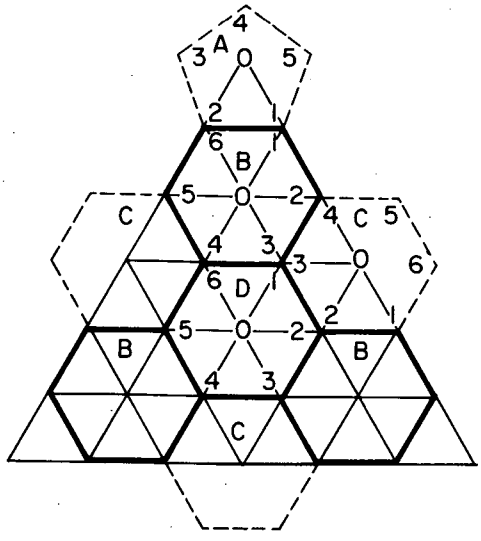

XBL 792-309

A12	0.24779	B12	0.18051	C12	0.20645	D12	0.20162
A23	0.24779	B23	0.20692	C23	0.20233	D23	0.20162
A34	0.24779	B34	0.20128	C34	0.20645	D34	0.20162
A45	0.24779	B45	0.20692	C45	0.20645	D45	0.20162
A51	0.24779	B56	0.18051	C56	0.20233	D56	0.20162
		B61	0.24695	C61	0.20645	D61	0.20162
A10	0.21078	B10	0.19316	C10	0.17070	D10	0.20162
A20	0.21078	B20	0.22604	C20	0.21914	D20	0.20162
A30	0.21078	B30	0.19292	C30	0.21914	D30	0.20162
A40	0.21078	B40	0.19292	C40	0.17070	D40	0.20162
A50	0.21078	B50	0.22604	C50	0.21914	D50	0.20162
		B60	0.19316	C60	0.21914	D60	0.20162

TABLE 4. Length of hexagons and pentagons of a polyhedron with 162 elements, having an inscribed touching sphere of unity.

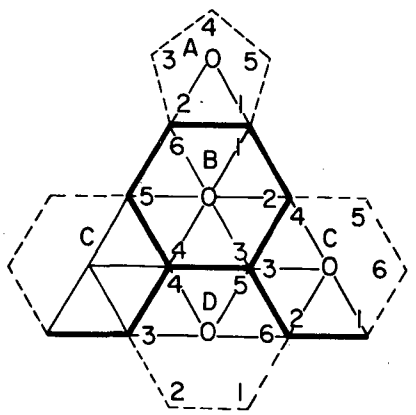

XBL 792-309

A12	0.21436	B12	0.17624	C12	0.19423	D12	0.17442
A23	0.21436	B23	0.16630	C23	0.17501	D23	0.17442
A34	0.21436	B34	0.17358	C34	0.16622	D34	0.17442
A45	0.21436	B45	0.16630	C45	0.16622	D45	0.17442
A51	0.21436	B56	0.17624	C56	0.17501	D56	0.17442
		B61	0.21428	C61	0.19423	D61	0.17442
A10	0.18234	B10	0.18000	C10	0.15055	D10	0.17442
A20	0.18234	B20	0.20783	C20	0.17596	D20	0.17442
A30	0.18234	B30	0.14331	C30	0.20455	D30	0.17442
A40	0.18234	B40	0.14331	C40	0.15055	D40	0.17442
A50	0.18234	B50	0.20783	C50	0.20455	D50	0.17442
		B60	0.18000	C60	0.17596	D60	0.17442

in a common edge, but rather in a common slip plane; that is, the edge is not quite at the same distance from the center of the polygons, and furthermore, the length of the sides of the touching crystals are no longer the same. Although these deviations are small, they must be considered in the actual design.

III. COMPONENTS OF THE CRYSTAL-BALL DETECTOR SYSTEM

1. The NaI(Tl) detectors

In the crystal ball, which approximates a sphere of radius 15 inches with a central spherical cavity of radius 9 inches, both the outer and inner surfaces are subdivided into 150 hexagons and 12 pentagons as specified in Table 3 of Section II. These 162 modules belong to four different three-dimensional shapes. The following numbers of modules make up the complete sphere:

Number of Modules	*Type of Module*	
12	A	regular pentagon
60	B	irregular hexagon
60	C	irregular hexagon
30	D	regular hexagon

Their drawings are compiled in the Appendix. While the NaI(Tl) crystals have a thickness of 6", the cans will be longer, with perhaps a length of 7", allowing for a wall thickness of about 1" at the outer hemisphere. These drawings define the critical outer dimensions and orientations of all faces of each module. The aluminum cans will probably be produced by folding and welding. Rather high mechanical tolerances have to be demanded for the cans, so that the modules, when packed together, reproduce the desired shell. We give here the same tolerances as for the Stanford crystal ball. The tolerances of the longitudinal dimensions of the modules are +0.000 inch and -0.015 inch, and the diameters of the different inscribed circles in the end faces are +0.000 inch and -0.005 inch. The tolerances of the flatness of the longitudinal sides of the modules are +0.000 inch and -0.005 inch. The tolerances on all dihedral angles are ±2.5 minutes of arc. All edges of each module are rounded

with a radius of 0.05 inch to prevent scratching of modules during assembly of the crystal ball. The crystals are hermetically sealed within an aluminum housing of 0.02" wall thickness at the inner and lateral faces. The thickness of the optical reflecting material is no more than 0.01". Each crystal is supplied with a feed-through for a LED, and is coupled to a selected RCA-4900 "teacup" 3-inch phototube. The phototube is enclosed within a mu-metal magnetic light shield and is terminated in a standard voltage divider.

Each crystal has a guaranteed energy resolution of 8% or better for Cs-137, independent of the position of the source. The shift in the detected photo-peak position is less than 1%, when changing the count-rate from 1 kHz to 70 kHz.

The prices for differently shaped crystals, including cans, photo-multipliers, and voltage dividers fulfilling these requirements, are estimates due to offers from Bicron Corp., Newbury, Ohio, and Harshaw Chemical Company, Solon, Ohio. The prices are compiled in Table 5, resulting in a total price of $332,000 for all detectors.

TABLE 5. Cost of Detector System

162 NaI(Tl) crystals (fabrication, encapsulation) Photo-tubes, light-pipes, mu-metal shields ($1482 per unit)	$241,000
162 cans and back plates ($562 per unit)	91,000
Total	$332,000

2. Mechanics

The individual counters of the crystal ball have to be kept in place by an outside support frame. In the Appendix, two technical drawings show a preliminary design study on the support frame. We want to use an aluminum sphere of 1.5-inch thickness and an inner diameter of 48 inches into which 162 portholes for the detectors are pierced with a large computer-driven mill. After preparing the portholes, the sphere is split into two vertical hemispheres. To each porthole an adjustable back plate is screwed. The detectors are held in place by a tube with a flange. Even when replacing a detector, the adjustment of the back plate is kept. This allows for an easy assembly of the whole system. The two hemispheres are carried by legs, which run on ball bearings in rails. The hemispheres can be separated to the left and right, to allow access to the central scattering chamber.

The scattering chamber will be a 1/8-inch-thick spherical aluminum chamber with an outer diameter of 17.5 inches. The small wall thickness and spherical shape are necessary to keep the absorption of γ rays as small as possible and to have a similar attenuation with respect to all detectors. We plan to divide the spherical chamber into three sections: a top lid, a central part, and a base part.

Price estimates for the design and construction of the support frame and the scattering chamber are compiled in Table 6.

TABLE 6. Mechanical costs.

Machine shop time for scattering chamber (300 hrs @ $19/hr)		$ 5,700
Fabrication of the supporting aluminum sphere with 162 portholes (900 hrs @ $30/hr)		27,000
Forging of sphere		9,000
Fabrication of adaptors and adjustment plates for 162 detectors (2000 hrs @ $19/hr)		38,000
Fabrication of carriage, track and support legs (440 hrs @ $19/hr)		8,360
Design time for chamber and detector support (400 hrs @ $23/hr)		9,200
	Total	$97,260

3. Electronics

From the crystal ball we shall obtain a linear energy signal from each of the counters that fires during an event, and also a summed or total energy signal. We shall also obtain a time signal from each counter that fires which will be grouped with the corresponding energy signal, and a single multiplicity output, that is, a signal that indicates how many counters fired during that event. The main purpose of the time signal is to be able to discriminate neutrons from γ rays in the crystal ball counters by time-of-flight. But its application in isomer studies is evident. To decrease the amount of data actually stored on tape, a master gate will be required at the ADC's that is generated if both the total energy and the multiplicity are within certain limits.

A wideband gain-of-10 amplifier operating off the anode will be included with each phototube divider unit, and the output split to yield the linear energy signal and the timing signal. The former signal is divided again, one part going to a second gain-of-10 amplifier and then on to one channel of a multi-channel gated ADC. The other part goes to a resistor network which allows summing of the signals from eight counters and then goes to another gain-of-10 amplifier. For 162 counters there will be 21 such amplifiers; they are then summed in two fan-in-units to furnish the total-energy signal. This signal goes to an ADC and is also branched through a discriminator. The output of the discriminator is put in coincidence with a similar gate from the multiplicity unit (see below) to make a master gate for all the ADC's.

The timing signal from each counter goes to one channel of a multi-channel constant-fraction discriminator. Two outputs are taken from the

discriminator. One goes to a 32-channel multiplicity logic unit which gives an output whose amplitude is proportional to the number of simultaneous inputs received. The six such units necessary to accommodate 162 channels can be further summed together in a fan-in unit, and the resulting multiplicity signal is branched, one signal going to an ADC for processing as the event multiplicity, and the other to a discriminator. The latter signal in coincidence with the already described total-energy gate makes up the master gate for the ADC's.

The second timing signal from the constant-fraction discriminator goes to a fast overlap coincidence unit which is also supplied by either a machine rf pulse (at the SuperHILAC) or the output of a thin transmission plastic scintillator (at the 88" Cyclotron) to yield a pulse-length proportional to the time difference. This time signal is sent to the ADC into the channel next to its corresponding linear-energy signal, and can be used to decide whether that pulse is due to a γ ray or to a neutron.

The gain of the linear-energy signals is held constant by a H.V. controller which responds to the position of photo-diode pulses in the final γ-ray energy spectrum.

Most of the electronic units will be purchased commercially. The major exception is the multi-channel constant-fraction unit which will be produced here, but will have been built and used at the Bevalac well before it is needed here. The costs for the electronics for a crystal ball with 162 units is compiled in Table 7.

TABLE 7. Electronics for the Crystal Ball.

Unit	Company	Item	Channels per unit	Number units	Cost per unit	Total ($)
HV4035	LRS	HV power supply; computer controlled, 2 mA and 3 kV	32	6	4750	28,500
2132	LRS	HV to Camac interface	--	1	450	450
VV100B	LRS	Wideband Pulse Amplifier for Photo-multiplier; 10x gain, risetime <2 nsec, ±0.1% integral linearity	--	350	34	11,900
AA100BL	LRS	VV100B Amplifier mounting board for testing	--	1	86	86
127FL	LRS	Dual bipolar linear fan-in	16	4	425	1,700
2285A	LRS	ADC 200 μs digitizing time, 12 bits, charge integrating	24	15	1585	23,775
2280	LRS	ADC System Processor; pedestal correction, zero suppression	--	1	2500	2,500
DK-6/50	LRS	Multicoax ribbon cable delay (100 nsec) [$35(connectors) + .65¢ x feet]	6	28	48	1,344
--	Home-built	Octal constant fraction discriminator, 2 out-puts, LED indicator, & overlap coincidence unit	8	21	~1200	25,200
380A	LRS	Multiplicity Logic Unit; no strobe signal, generates master trigger, analog multi-plicity output	32	6	895	5,370
821	LRS	Quad 100 MHz Discriminator for multiplicity and total energy gates	4	1	825	825
365AL	LRS	Dual 4-fold Majority Logic Unit; generates master gate	2	1	715	715

Electronics for Crystal Ball (continued)

Unit	Company	Item	Channels per unit	Number units	Cost per unit	Total ($)
429A	LRS	Fan-out for master gate	16	2	529	1,058
2551	LRS	12-channel, 24-bit, 100 MHz Scaler		1	575	575
108P-6	LRS	NIM power chassis (±12V, ±24V, ±6V)		4	810	3,240
Ultima 3000	Standard Engineering	CAMAC Crate		2	2000	4,000
		CAMAC crate controller		2	2000	4,000
		Cables and connectors				25,000
						$140,238

IV. LOGISTICS

1. Time schedule

In summer 1979, a sub-unit consisting of one central detector with a pentagonal end-face surrounded by five hexagonal detectors can be ordered and then tested. The aim is to study the properties (response function, timing, etc) of an individual detector and the Compton scattering between detectors. This check of the predicted properties of the detectors allows for a final optimization of the design. At the same time, electronics and first software programs can be developed.

This unit will be useful in its own right as a Compton-suppressed or Compton-added spectrometer. If this proposal is accepted, the total NaI system could be ordered October, 1980; delivery of the canned NaI(Tl) detectors and phototubes by Harshaw Chemical Company of Solon, Ohio, or Bicron Corp. of Newbury, Ohio, is guaranteed within 6-9 months. About the same delivery time exists for the commercial electronics (Le Croy). Thus, first tests of the system could be performed in Summer-Fall 1981. This is likely to be at the 88" Cyclotron, studying primarily compound nuclear reactions, as these studies would emphasize the γ-ray measurements and not require any coincident particle counters. When some familiarity is achieved with the crystal ball, it will be moved to the SuperHILAC for more complicated deep-inelastic reaction studies, observation of high-energy non-equilibrium particles, transfer reactions of heavy ions with simultaneous Coulomb excitation, etc.

2. Budget

Table 8 lists all major anticipated costs. It is subdivided into the NaI(Tl) detectors, mechanics, and electronics.

Only the purchase of the complete NaI(Tl) detectors (crystals, cans and phototubes) allows for guarantees of energy resolution, count-rate stability, and most importantly, the hermeticity of the cans and required mechanical tolerances.

The mechanical cost consists predominantly of the support frame for the 162 crystals, while the price for the thin spherical scattering chamber is relatively low. The cost of the support frame is divided about equally into the basic aluminum support sphere with legs and carriage, and the many adaptors and adjustment plates for the individual crystals.

The electronics consists predominantly of commercial units. The home-built units are octal constant-fraction triggers. A quadruple model is already in use and allows a rather good estimate of the price for the octal unit, which is being designed for another purpose already.

These costs are as of March, 1979, and, depending upon the time of actual construction, will have to be increased for inflation.

TABLE 8. Total cost estimates for the Crystal Ball.

Detectors (details, Table 5)	$332,000
Mechanics (details, Table 6)	97,260
Electronics (details, Table 4)	140,238
Contingencies (5%)	30,000
Grand Total	$599,498

REFERENCES

1. J.J.Simpson, P.O.Tjøm, I.Espe, G.B.Hagemann, B.Herskind, and M.Neiman, Nucl. Phys. A287, 362 (1977).

2. P.O.Tjøm, I.Espe, G.B.Hagemann, B.Herskind, and D.L.Hillis, Phys. Lett. 72B, 439 (1978).

3. R.S.Simon, M.V.Banaschik, R.M.Diamond, J.O.Newton, and F.S.Stephens, Nucl. Phys. A290, 253 (1977).

4. M.A.Deleplanque, Th.Byrski, R.M.Diamond, H.Hübel, F.S.Stephens, B.Herskind, and R.Bauer, Phys. Rev. Letters 41, 1105 (1978).

5. W.Trautman, J.deBoer, W.Dünnweber, G.Graw, R.Kopp, C.Lauterbach, H.Puchta, and U.Lynen, Phys. Rev. Letters 39, 1062 (1977).

6. M.Berlanger, J. Phys. (Paris) Letters 33, 1323 (1976).

7. P.Dyer, R.J.Puigh, R.Vandenbosch, T.D.Thomas, and M.S.Zisman, Phys. Rev. Letters 39, 392 (1977).

8. H.Ho, R.Albrecht, W.Dunnweber, G.Graw, S.G.Steadman, J.P.Wurm, D.Disdier, V.Rauch, and F.Scheibling, Z. Phys. A283, 235 (1977).

9. H.J.Specht, invited talk at the International Conf. on Nuclear Interactions, Canberra, Australia (August, 1978).

10. M.A.Deleplanque, I.Y.Lee, F.S.Stephens, R.M.Diamond, and M.M.Aleonard, Phys. Rev. Letters 40, 629 (1978).

11. G.B.Hagemann, R.Broda, B.Herskind, M.Ishihara, S.Ogaza, and H.Ryde, Nucl. Phys. A245, 166 (1975).

12. P.O.Tjøm, F.S.Stephens, R.M.Diamond, J.deBoer, and W.E.Meyerhof, Phys. Rev. Letters 33, 593 (1974).

13. R.Partridge et al., Proposal PEP-18, Stanford University (October 1977).

14. D.G.Sarantites, "A Nuclear-Spin Spectrometer," proposal submitted to the U.S. Dept. of Energy, 1978.

15. K.Siegbahn, Alpha-, Beta-, and Gamma-Ray Spectroscopy (North-Holland Publishing Co., Amsterdam, 1974).

16. J.R.Stehn, M.D.Goldberg, B.Magurno, R.W.Chasman, Neutron cross sections, Report BNL-325 (Brookhaven National Laboratory, 1964).

17. J.O.Newton, I.Y.Lee, R.S.Simon, M.M.Aleonard, Y.El Masri, F.S.Stephens, and R.M.Diamond, Phys. Rev. Letters 38, 810 (1977).

18. Anthony Pugh, Polyhedra: A Visual Approach (Univ. of California Press, 1976).

APPENDIX

TECHNICAL DRAWINGS OF THE CRYSTAL BALL

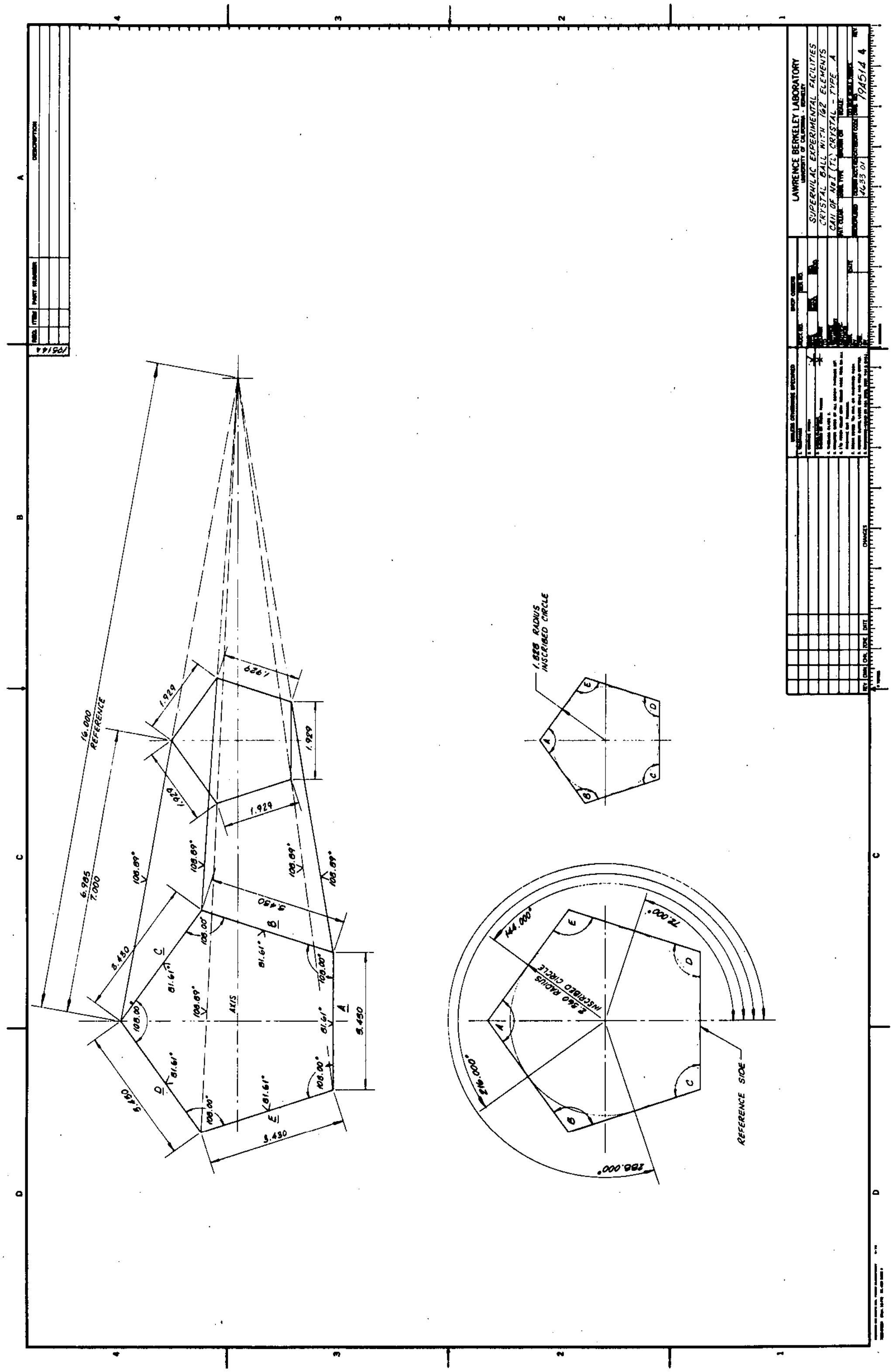
LAWRENCE BERKELEY LABORATORY
SUPERHILAC EXPERIMENTAL FACILITIES
CRYSTAL BALL WITH 162 ELEMENTS
CELL OF NaI (Tl) CRYSTAL - TYPE A
19A514 A
16.000 REFERENCE
6.985
7.000
1.929
5.450
108.00°
81.61°
105.00°
AXIS
1.888 RADIUS INSCRIBED CIRCLE
2.560 RADIUS INSCRIBED CIRCLE
REFERENCE SIDE
72.000°
144.000°
216.000°
288.000°

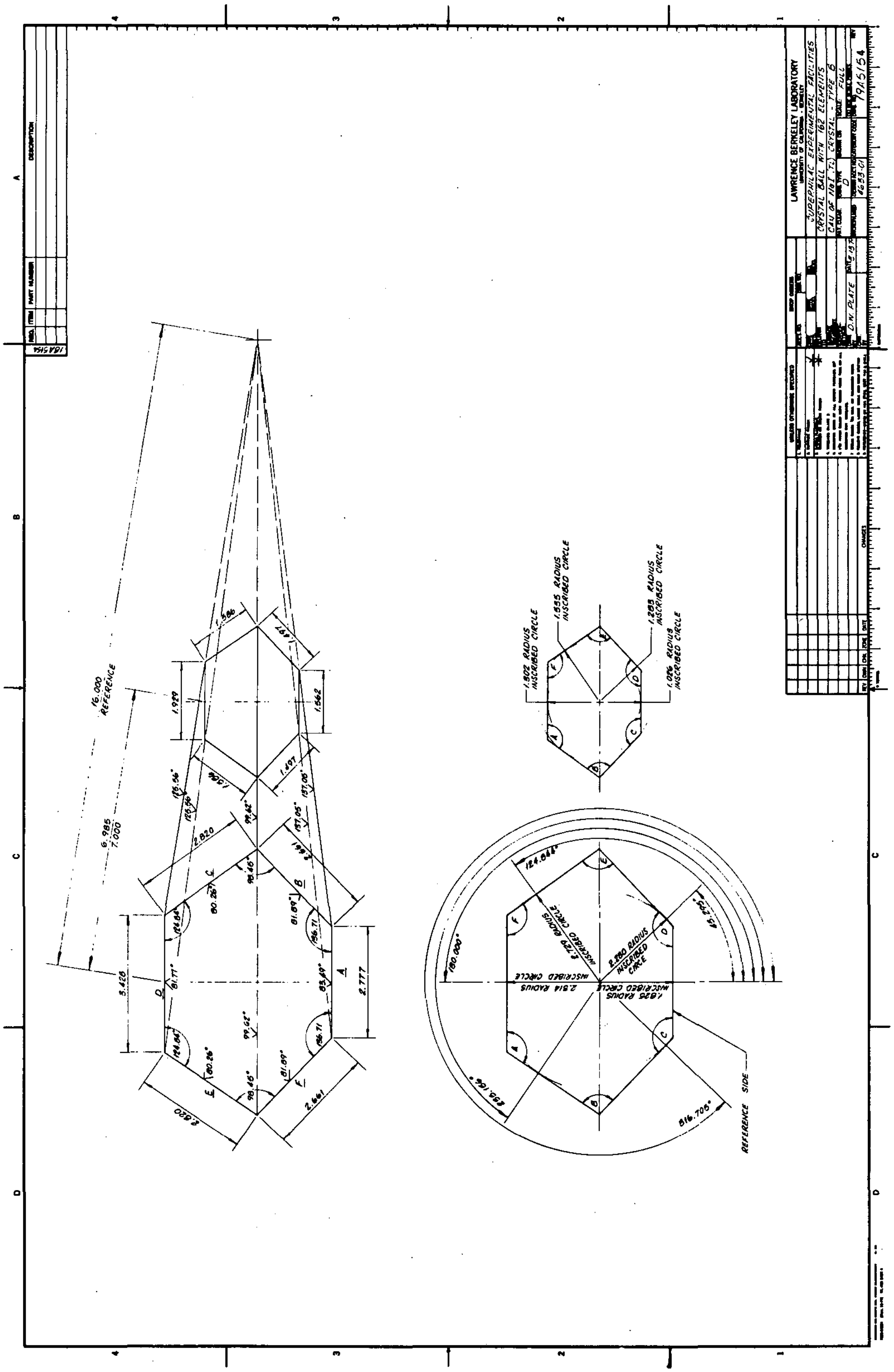

LAWRENCE BERKELEY LABORATORY
SUPERHILAC EXPERIMENTAL FACILITIES
CRYSTAL BALL WITH 162 ELEMENTS
16.000 REFERENCE
REFERENCE SIDE
1.802 RADIUS INSCRIBED CIRCLE
1.555 RADIUS INSCRIBED CIRCLE
1.283 RADIUS INSCRIBED CIRCLE
1.026 RADIUS INSCRIBED CIRCLE
2.980 RADIUS INSCRIBED CIRCLE
2.514 RADIUS INSCRIBED CIRCLE

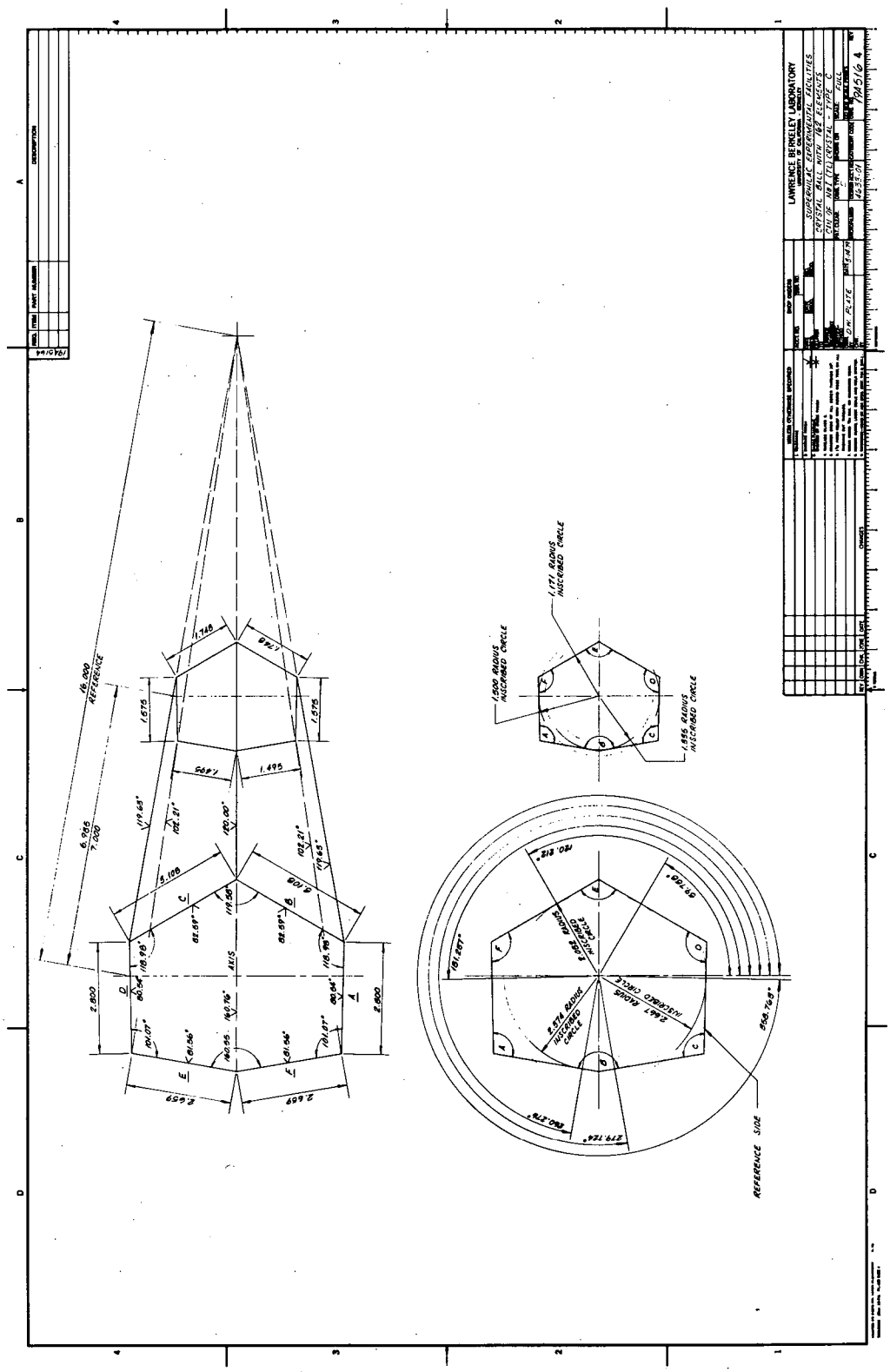
LAWRENCE BERKELEY LABORATORY
UNIVERSITY OF CALIFORNIA, BERKELEY
SUPERNULAR EXPERIMENTAL FACILITIES
CRYSTAL BALL WITH PE ELEMENTS
1945164
1.748
1.575
1.495
16.000 REFERENCE
6.926
7.000
5.109
2.800
2.659
1.500 RADIUS INSCRIBED CIRCLE
1.171 RADIUS INSCRIBED CIRCLE
1.886 RADIUS INSCRIBED CIRCLE
2.667 RADIUS INSCRIBED CIRCLE
2.574 RADIUS INSCRIBED CIRCLE
REFERENCE SIDE

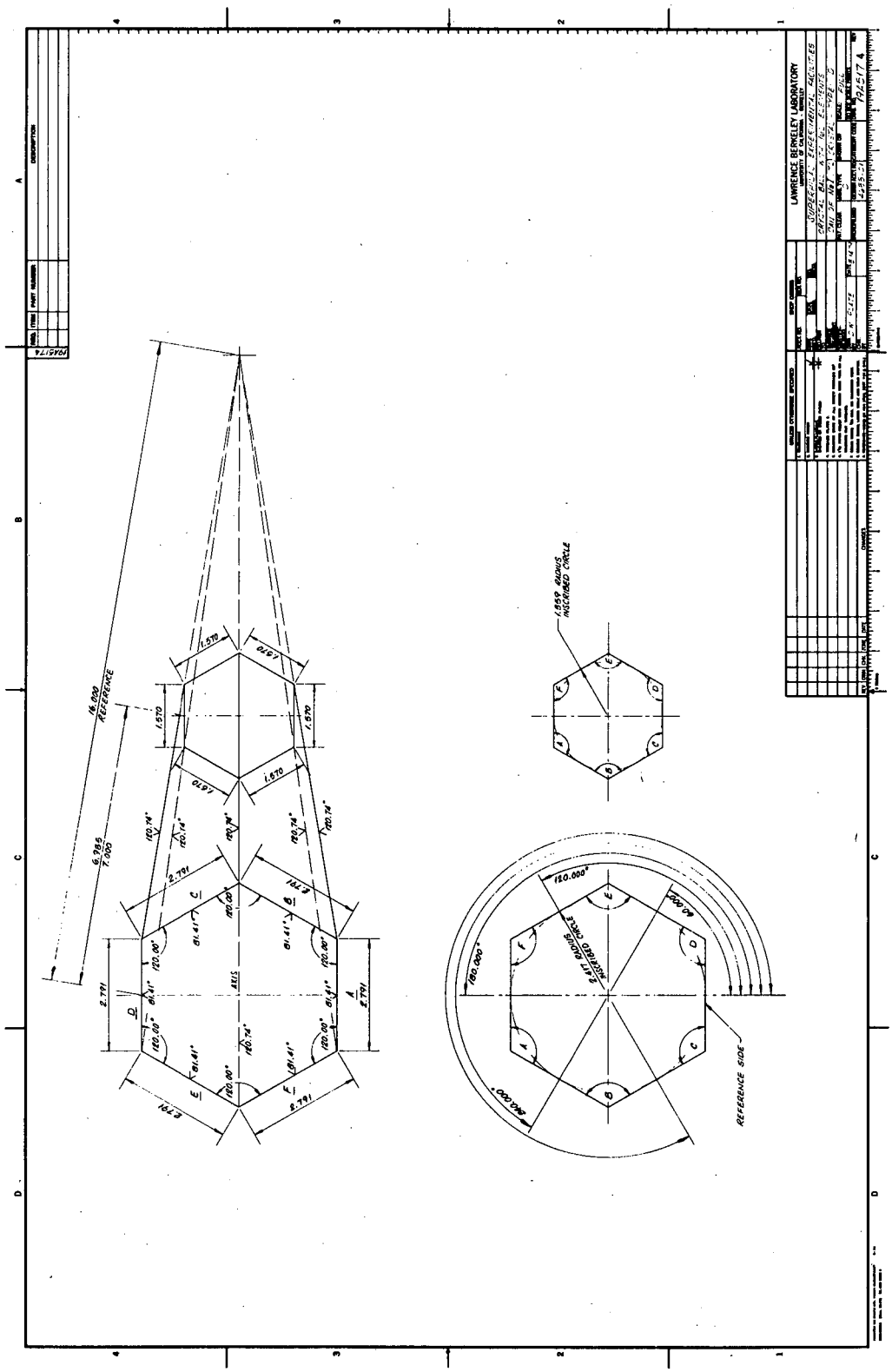
LAWRENCE BERKELEY LABORATORY
1.570
2.791
120.00°
120.74°
91.41°
180.000°
REFERENCE SIDE

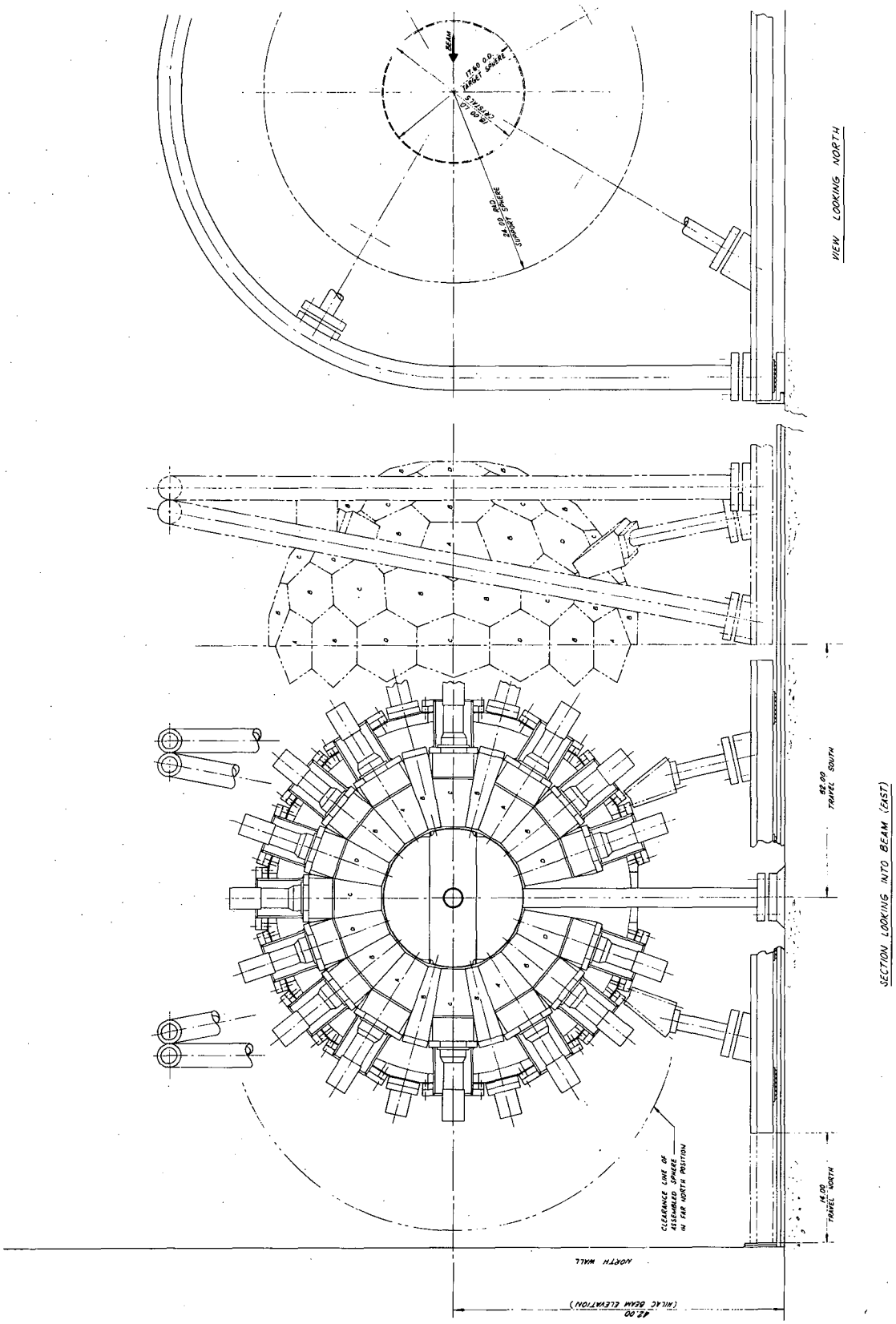

SUPERHILAC EXPERIMENTAL FACILITIES
CRYSTAL BALL WITH 122 ELEMENTS
PROPOSED CRYSTAL BALL MOUNTING

SCALE: 1/4
DRAWN AUGUST 4833-C1
SCANNED BY TIF PLOTTER 2-10-79

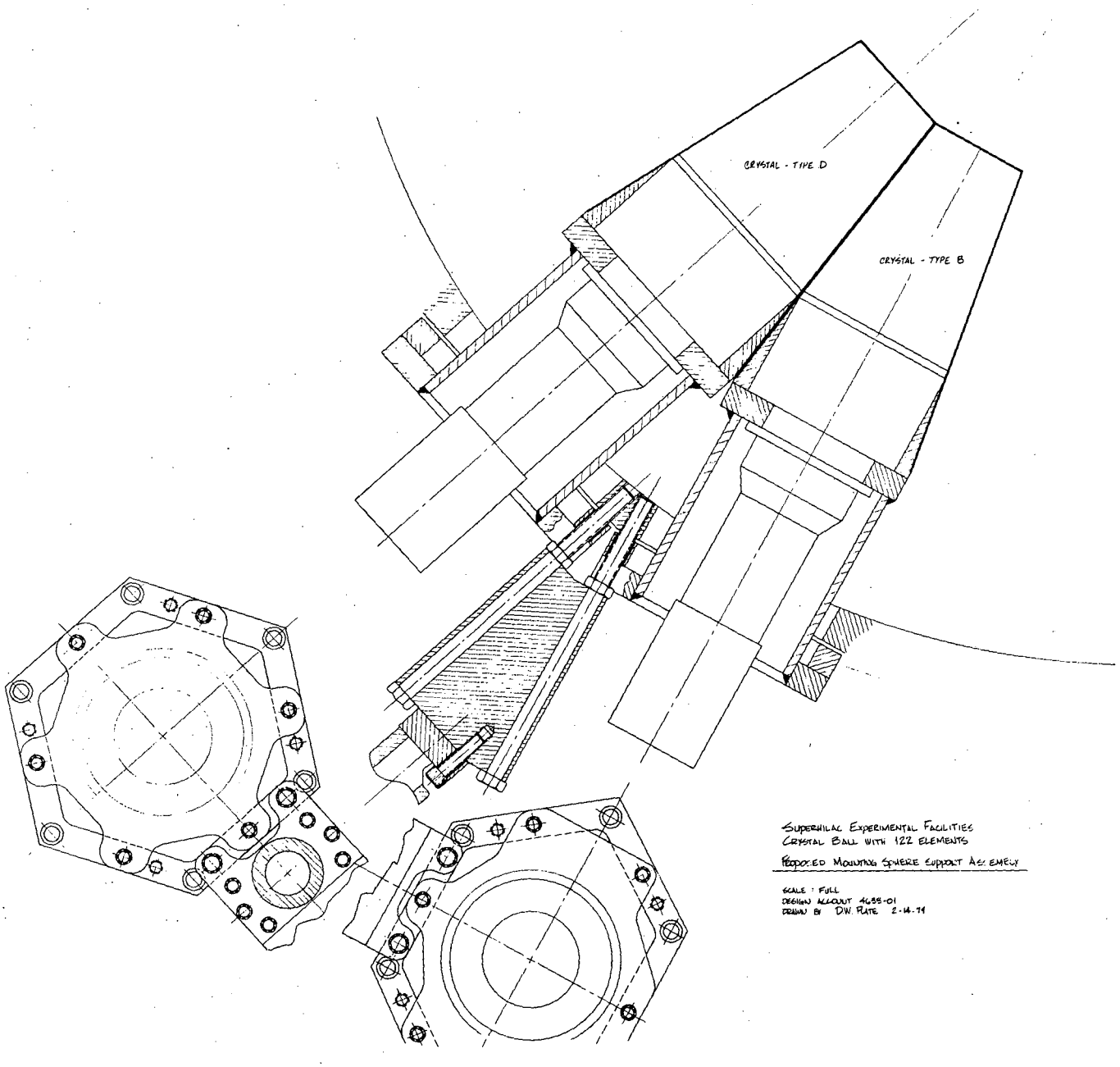

SUPERHILAC EXPERIMENTAL FACILITIES
CRYSTAL BALL WITH 122 ELEMENTS
PROPOSED MOUNTING SPHERE SUPPORT ASSEMBLY

SCALE : FULL
DESIGN ACCOUNT 4655-01
DRAWN BY D.W. PLATE 2-14-74

U.S.GPO:1979-689-058(F)15

TECHNICAL INFORMATION DEPARTMENT
LAWRENCE BERKELEY LABORATORY
UNIVERSITY OF CALIFORNIA
BERKELEY, CALIFORNIA 94720